

國立交通大學

資訊學院 資訊學程

碩士論文

一個針對行人位置推估系統的

速度校正方法



**A Walking Velocity Update Technique for Pedestrian  
Dead-Reckoning Systems**

研究生：邱正平

指導教授：曾煜棋 教授

中華民國一百年十月

一個針對行人位置推估系統的速度校正方法  
A Walking Velocity Update Technique for Pedestrian  
Dead-Reckoning Systems

研究生：邱正平

Student : Chen-Ping Chiu

指導教授：曾煜棋

Advisor : Yu-Chee Tseng

國立交通大學

資訊學院 資訊學程



Submitted to College of Computer Science

National Chiao Tung University

in partial Fulfillment of the Requirements

for the Degree of

Master of Science

in

Computer Science

June 2011

Hsinchu, Taiwan, Republic of China

中華民國一十年十月

# 一個針對行人位置推估系統的速度校正方法

學生：邱正平

指導教授：曾煜棋

國立交通大學

資訊學院

資訊學程

碩士班

## 摘 要

隨著微機電技術的日新月異，各式低價、體積又小的慣性感應器已大量出現。使用慣性感應器應用於行人導航上已在最近引起各方的注意。在行人慣性導航的方法中，對慣性感應器所測到的加速度作二次積分，來推估位置是最直接有效的方法，但前提是需能夠克服因感測器精度不足，加速度在對時間積分後快速產生的累計誤差，在過去可將感測器安裝在足部利用 ZUPT 的技巧，在行走過程中足部著地時速度大小應為零的特性，來校正行人導航的速度，但此方法限制是需將感測器安裝在足部，而行走過程中足部運動的變化非常劇烈，反而有感測器量測誤差擴大的副作用，特別是前進方向上的量測上。現在本研究提出另外一種累計誤差的校正方法，並可避免量測誤差的擴大，該方法稱作 Walking velocity update 簡稱 WUPT，該方法使用 2 組感測器，一組安裝在軀幹上，因上半身的運動變化較不劇烈，可量測到較可靠的前進方向和加速度，使 PDR 系統進而推估出較準確的行人速度和位移，另一組 sensor 安裝在小腿上量測角速度，於行進中該腿垂直站立於地，大小腿幾無相對運動的時刻，透過牛頓運動定律反推上半身應有的正確速度，來校正系統的推估速度。我們已利用該方法實作出新型的行人慣性導航系統，經驗證該系統的定位性能的確優於 ZUPT PDR 系統。

**關鍵字：**行人慣性導航、行人位置推估、慣性量測單元、慣性感測器、個人定位

# **A Walking Velocity Update Technique for Pedestrian Dead-Reckoning Systems**

student : Chen-Ping Chiu

Advisors : Dr. Yu-Chee Tseng

Degree Program of Computer Science

National Chiao Tung University

## **ABSTRACT**

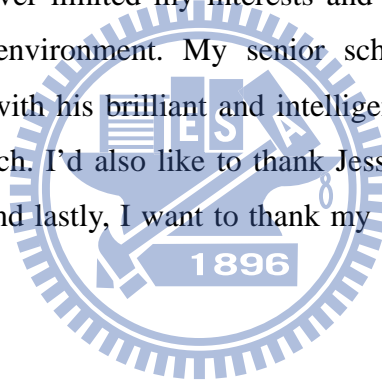
Along with the MEMS technology development, there are various low-cost and small-volume inertial sensors produced massively. Using inertial sensors for Pedestrian Dead-reckoning has attracted a lot of attention recently. It is the most efficient and direct way to estimate the displacement by using the integration of acceleration, but the prerequisite is to overcome the increase of the accumulated error with time rapidly. In the past, there was a famous ZUPT technique, whereby the researchers installed the sensor on the pedestrian's foot and corrected the speed of the PDR system by using the characteristic, which is that the speed of the foot is zero while the foot is landing on the ground during the movement. The limit of this method is that the sensor has to be installed on the foot. The side effect of the sensor placement on the foot is that the dramatic movement would extend the sensor measurement error, especially for the heading determination. The contribution of this thesis is to propose another kind of correction method for the accumulated error and avoid the disadvantage of the ZUPT technique. This kind of correction method is called the WUPT technique, short for the Walking Velocity Update. The technique uses two sets of the inertial sensors on the pedestrian. One set is installed on the torso due to more stability of the movement, so we can obtain a more accurate measurement of the heading direction and the acceleration. The other set is installed on the pedestrian's low leg to measure the angular rate. We can correct the estimate speed of the torso with the angular rate of the low leg at the moment the thigh and the low leg become a straight line vertical to the ground during the walking. We have used this method to make the WUPT PDR system prototype and have verified that its localization performance is superior to the ZUPT PDR system.

**Keywords:** ZUPT, WUPT, PDR, Pedestrian Dead-reckoning, IMU, inertial measurement unit, inertial sensor, personnel navigation system, localization, positioning



# Acknowledgements

I've been working at the industry of Information and Electrical field since I graduated from university. I always consider myself as an outsider because I've never received any course which is related to Information and Electrical Engineering. The idea of going back to school to improve my professional knowledge and skills occurred to me ten years ago. I decided to attend the Extended Education on Information and Electrical Engineering Master Program in National Chiao Tung University, and finally, I realized my dream before turning to forty years old. I feel an immense gratitude to those people for helping me make my wish come true. I'd like to thank my current company, Princo Corporation. They not only offer me a job keeping a family but also encouraged me to go to graduate school. I especially want to thank my wife, Yu-Ting. Without her incredible support, my dream would never have become a reality. There are another two individuals who helped me with my thesis that deserve special thanks. My advisor, Yu-Chee Tseng, never limited my interests and gave me all his support, including finance and the research environment. My senior schoolmate from the doctoral class, Chi-Chung Lo, helped me with his brilliant and intelligent opinions when I was confronted with problems in my research. I'd also like to thank Jessica Jongedik, who helped me with emendation to my thesis. And lastly, I want to thank my son, Hsin-Yuan, who is the light of my life.



Chen-Ping Chiu

May, 2011 in Hsinchu, Taiwan

# Contents

<b>Abstract</b>	i
<b>Acknowledgements</b>	iv
<b>Table of Contents</b>	v
<b>List of Figure</b>	vi
<b>List of Table</b>	vii
<b>1 Introduction</b>	<b>1</b>
<b>2 Related Work</b>	<b>3</b>
<b>3 Problem Definition</b>	<b>8</b>
<b>4 Methodology</b>	<b>9</b>
4.1 Coordinate Systems and Transformations	10
4.1.1 Local Level Frame	10
4.1.2 The Body Frame	11
4.1.3 The Sensor Frame	12
4.1.4 Coordinate Frame Transformation	12
4.2 WUPT Technique	16
4.3 WUPT PDR System Architecture	19
4.2.1 Stride Detection Block	20
4.2.2 Walking Velocity Update Block	22
4.2.3 Location Tracking Block	22
<b>5 Implementation and Experimentation</b>	<b>24</b>
5.1 Implementation	24
5.2 Experimentation	27
5.2.1 Experiment 1 - The Basic Route Test	28
5.2.2 Experiment 2 – The Square Route Test	31
5.2.3 Experiment 3 - The Circle Route Test	34
5.2.4 Experiment 4 - The Practical Outdoor Positioning Test	37
5.2.5 Experiment 5 - The Practical Indoor Positioning Test	39
<b>6 Conclusion</b>	<b>42</b>
<b>References</b>	<b>43</b>
<b>Biography</b>	<b>45</b>

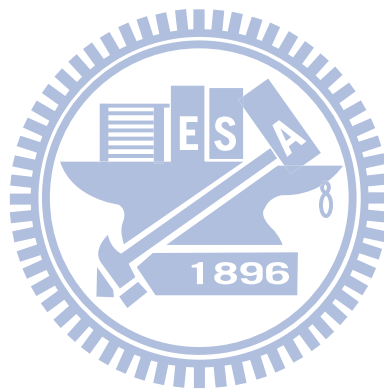
# List of Figures

Figure 2-1 comparison of acceleration according to two strides	4
Figure 2-2 compass signal comparison	6
Figure 2-3 acceleration magnitude comparison	6
Figure 4-1 placement of inertial sensor Sb and Sl	9
Figure 4-2 local level frame	10
Figure 4-3 body frame	11
Figure 4-4 rotation 1	13
Figure 4-5 rotation 2	14
Figure 4-6 rotation 3	15
Figure 4-7 kinematics model of human walking in mid-stance	16
Figure 4-8 the motion curve of knee	17
Figure 4-9 function block of WUPT PDR	19
Figure 4-10 A stride cycle of human walking	20
Figure 4-11 a chart of pitch angle and angular rate of low leg with time	21
Figure 5-1 3DM-GX1	25
Figure 5-2 Sb placement	25
Figure 5-3 Sl placement	25
Figure 5-4 WUPT PDR	25
Figure 5-5 read3DMGX1.vi	26
Figure 5-6 analysis.vi	27
Figure 5-7 trajectory of the basic test	28
Figure 5-8 estimated velocity before and after WUPT update	29
Figure 5-9 the measurement of heading direction on straight line at slow speed	30
Figure 5-10 the measurement of heading direction on straight line at high speed	30
Figure 5-11 trajectory of WUPT of the Square Route test	32
Figure 5-12 trajectory of ZUPT of the Square Route test	33
Figure 5-13 trajectory of WUPT of the Circle Route test	35
Figure 5-14 trajectory of ZUPT of the Circle Route test	36
Figure 5-15 trajectory of the Practical Outdoor Positioning Test	38
Figure 5-16 trajectory of Route 1 of the Practical Indoor Positioning Test	40
Figure 5-17 trajectory of Route 2 of the Practical Indoor Positioning Test	41



## List of Tables

Table 5-1 3GM-DX1 spec	24
Table 5-2 results of the basic test	28
Table 5-3 results of WUPT of the Square Route test	32
Table 5-4 results of ZUPT of the Square Route test	33
Table 5-5 results of WUPT of the Circle Route test	35
Table 5-6 results of ZUPT of the Circle Route test	36
Table 5-7 results of the Practical Outdoor Positioning Test	37
Table 5-8 results of Route 1 of the Practical Indoor Positioning Test	39
Table 5-9 results of Route 2 of the Practical Indoor Positioning Test	41



# Chapter 1

## Introduction

Recently, a lot of location-based services (LBS) [3], [4], such as navigation and tracking, have been proposed. A central issue in LBS is location tracking. At present, GPS is still the widest used technology for positioning in outdoor environments. However, due to shadowing effects, GPS is not always available or even reliable. Therefore, lots of efforts have been dedicated to alternative positioning techniques. Those techniques can be classified into six categories: AoA-based [5], ToA-based [6], TDoA-based [7], signal loss-based [8], pattern-matching [9], [10], [11], and pedestrian dead-reckoning [1], [2], [12], [13], [14], [16] techniques. In this thesis, we are interested in PDR systems that rely on inertial sensors, such as an accelerometer, an electronic compass, and gyro sensors mounted on a human body (which can measure accelerations, orientations, and rotations respectively) to track the user's location. PDR concepts come from DR, which is a technique very widely used in navigation of vehicles or boats. DR devices are expensive and bulky, so it's not suitable to be applied in pedestrian navigation. Along with the MEMS technology development, there are various low-cost and small-volume inertial sensors produced massively. Today these tiny sensors have been used in pedestrian navigation. PDR has been proposed for a large range of applications, such as defense, emergency rescue works, smart offices, and so on. The simplest PDR system is the pedometer, which counts steps. However, a walking motion is composed of a series of strides. By triaxial accelerometer and e-compass sensors, we can better characterize a stride. In [12], a pattern matching method is used for detecting strides from vertical accelerations. In [13], the step event is detected by the cooperation of a vertical accelerometer and the angular rate of the user's ankle axis. In [14], regression analysis is applied to detect the walking frequency and the variance of accelerometer signals during one step. A conversion equation between stride length and step duration is derived. However, these systems all produce large errors when a user moves in a way other than his/her normal walking patterns. In order to reduce measurement errors, one fundamental issue in PDR systems is to find a good way to calibrate the system. The main reason is that accelerometers may accumulate lots of errors when the information is converted to speeds and displacements. In order to relieve the error drifting problem, a technique known as ZUPT (Zero Velocity Update) has been proposed [1], [2], [16].

The main idea of ZUPT is to use a foot-mounted inertial sensor. It is claimed that this sensor's reading should be close to zero when the sole of the foot touches the ground. This event is a good moment to calibrate the system, i.e., we can reset the user's walking velocity to zero when the system predicts the happening of such an event. The main drawback of ZUPT is that the inertial sensor needs to be mounted on the very bottom of a foot, thus leading to a lot of vibrations and errors when measuring orientations and displacements. Our objective is to find another way to effectively remove both accumulated errors and orientation errors. A new concept called "Walking Velocity" Update (WUPT) is proposed, where we use an inertial sensor mounted on the lower leg to find proper timing to calibrate the user's walking velocity and send this feedback to another sensor mounted on the upper body. The former is to calibrate the latter and the latter actually measures the user's velocity and orientation by continuously receiving feedbacks from the former. Our results are based on the following observations concerning walking motions. First, the angular velocity with respect to the ground of the lower leg may reflect the current walking velocity of a person when his/her upper and lower leg form a straight line. Second, when the aforementioned straight line is vertical to the ground (i.e., its pitch value = 0), the angular rate can be converted to the body velocity quite accurately. Third, mounting an inertial sensor on the upper body or torso incurs less position errors than mounting one on the foot for the purpose of trajectory tracking. A prototype has been developed to verify our claims. The rest of this thesis is organized as follows. Chapter 2 expresses the related works of PDR. Chapter 3 defines the problem we are solving. Chapter 4 presents our idea and detailed approach. Chapter 5 illustrates our implementations and experimental results. Chapter 6 concludes the thesis.

# Chapter 2

## Related Works

By traditional DR method to calculate displacement over time, it's impossible to track position for more than a few seconds by using low-cost inertial sensing alone. Even a tiny drift rate in the gyros will cause a slowly growing tilt error. Further explanation, the horizontal acceleration error is  $9.8 \text{ m/s}^2$  times the tilt error in radians. Double integrating this increasing acceleration error will produce a position error that grows cubically in time in the short term. Thus, the small inertial sensors can maintain accuracy of a few millimeters for one second, but the drift will exceed more than one meter in 10 seconds [1]. Today, all the Pedestrian Dead-Reckoning (PDR) solutions integrate step detection, step lengths and orientation estimations at each step, as to compute the absolute position and orientation of a person. By that we can easily break the position error with time cubed into with steps.

In the past, Weinberg demonstrated how to obtain the final location of the pedestrian [17]. By putting a pedometer, which is assembled by an electrical compass and a z-axis accelerometer on the waist belt, the strides can be detected by the changes of the signals of z-axis accelerometer that is produced while the pedestrian's center of gravity is moving up and down in walking. The length of stride is proportional to the bounce or vertical movement of the human hip. This hip bounce is estimated from the largest acceleration differences at each step. The stride is inferred as:

$$\text{Stride} = K \{ A_{\max} - A_{\min} \}^{1/4}$$

$A_{\max}$  is the maximum of acceleration on z-axis,  $A_{\min}$  is the minimum of acceleration on z-axis, and K is a constant. The orientation of the stride is measured by an electrical compass. Eventually the final location the pedestrian is obtained by summing up all strides.

The PDR system [18] places IMU on the lower leg, near the ankle. It uses an inertial measurement unit (IMU), which consists of a double-axial accelerometer, a single-axial gyroscope, and a single-axial electrical compass. The research observed that human walking gait consists of the swing phase when the heels are off the ground and the stance phase when the heels are on the ground, which take place in turn. During each period, the acceleration

components that are perpendicular and parallel to the lower leg have high-low/high-low variations (see Figure 2-1).

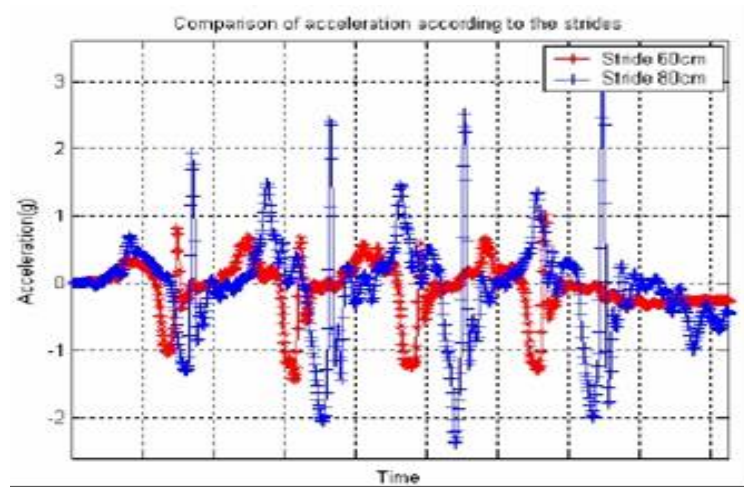


Figure 2-1 comparison of acceleration according to two strides

The author proposed a new step detect algorithm based on the analysis of vertical and horizontal acceleration of the foot during one step period of the walking. He found the stride is proportional to the height of the walker, the step frequency, and the walking velocity of the pedestrian, as below:

Stride	Mean value (g)
60cm	0.2882
80cm	0.5549

And the stride length is estimated as:

$$stride = 0.98 \sqrt[3]{\frac{\sum_{k=1}^N |A_k|}{N}}$$

N is total samples in one stride,  $A_k$  is the acceleration of the kth sample. And the orientation of the stride is determined by the compass and the gyroscope. The result of the experiment of the PDR system for straight line moving has only 1% of step detect error, 5% of distance error, and 5% of direction inaccuracy.

There are many Personal Dead-reckoning systems, which install the IMU on the foot (including heels of the shoes, the soles of the shoes and the insteps). The advantage of this is, compared to estimating strides with experience rules, it has better positioning performance and is more suitable for use according to the character of the total contact of the foot and the ground while standing, and to correct the errors of speed and position for the IMU with ZUPT technique.

In 2003, the first PDR using the ZUPT technique was proposed [16]. The system uses orthogonally-oriented circuit boards and each circuit board contains a double-axial accelerometer and a double-axial magnetometer to compose an inertial measurement unit and installs it on the shoe. System detects stride by taking the character that the IMU acceleration should be zero while the foot on the ground in walking. Also, get the distance and heading of the stride by double integrating the IMU horizontal acceleration. The error of the distance for PDR localization performance is around 15%, and the maximum error of heading is about 20 degrees. There is a special analysis for the advantages and disadvantages of the sensor placement on foot and torso in the paper. The advantage of putting a sensor on the torso is more stability to decide the heading and acceleration (see Figure 2-2, 2-3). The disadvantage is that it can't estimate the step length by acceleration integration. The advantage of putting a sensor on the foot is that it can estimate the step length by acceleration integration with ZUPT technique. The disadvantage is that it's more difficult for heading determination.

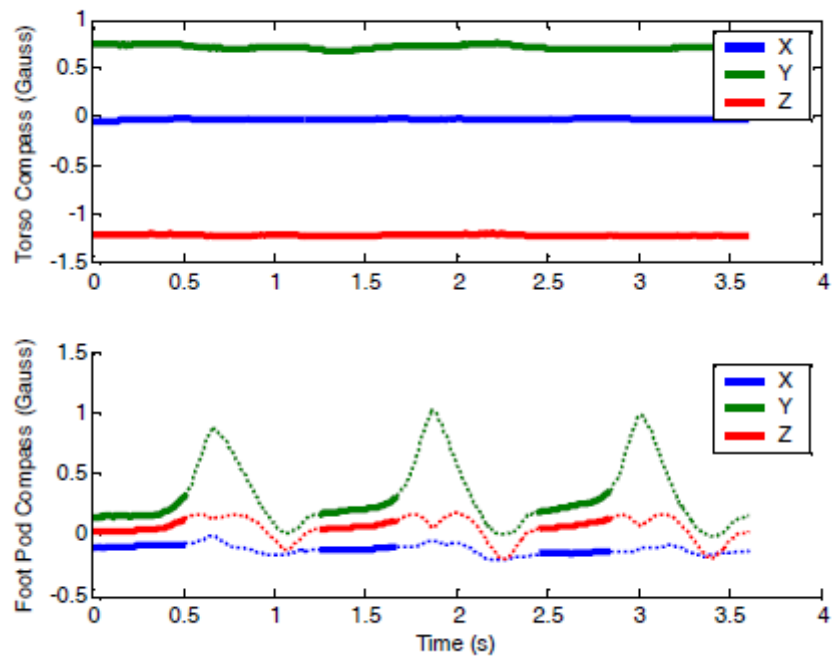


Figure 2-2 compass signal comparison on foot mounted and torso mounted

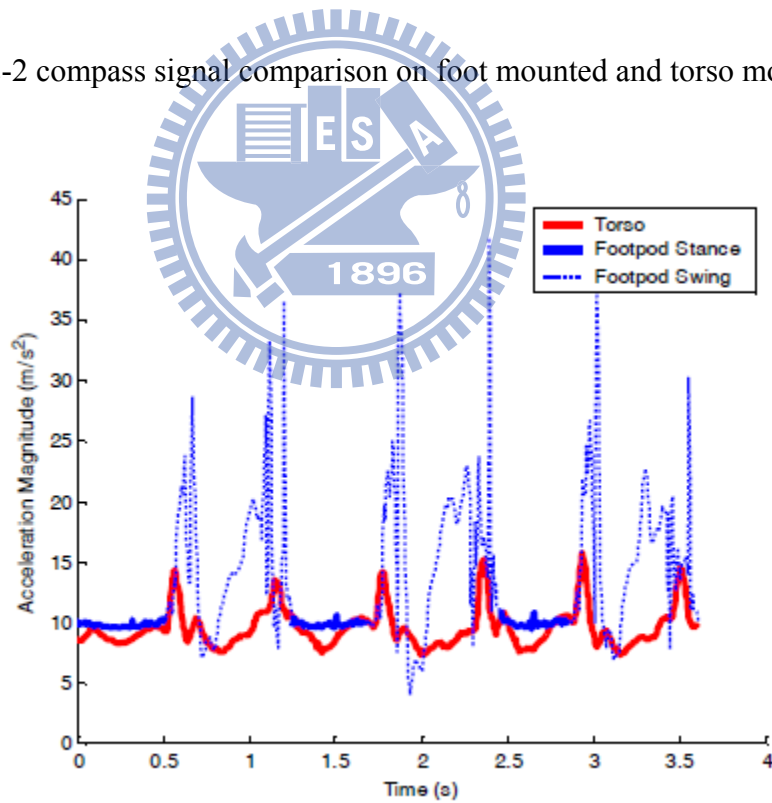


Figure 2-3 acceleration magnitude comparison on foot mounted and torso mounted

The most complicated PDR system is performed [19], which is assembled by two sets of the PDR systems. One of them is to install the IMU on the foot in order to get more accurate

results of the distance and a better and wider usage by using the typical ZUPT technique. The other is to install the IMU on the torso, combined with a laser range finder and vision to estimate stride length with experience rules because of the more accurate heading determination and better results of tracking exquisite routes. The result of combining two PDR systems is to get the most accurate and useful PDR localization system in order to use it in the rescue sites accurately and functionally.

According to the survey of the PDR system with the IMU on the foot and the ZUPT technique [15], the PDR positioning accuracy depends on the algorithm implemented, environment and inertial sensor technology employed, normally ranges from 0.5% to 10% of the total traveled distance. The main source of positioning errors is the absolute orientation estimation due to the big movement of the IMU on foot.

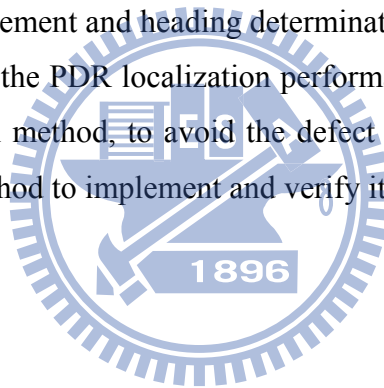
There is some work to research the sources of the PDR positioning errors. In [20] it pointed out that the low-cost MEMS gyroscopes work on the basis of Coriolis Effect. A severe limitation of Coriolis-based gyroscopes is that they are sensitive to linear acceleration normal to the measurement axial of gyroscope. The acceleration of swing phase is changed dramatically on foot, which seriously affects the accuracy of positioning. It is more accurate for measuring the orientation by the torso-mounted IMU than the foot-mounted. This thesis is to aim at the above-mentioned ZUPT defect to propose a better solution.



# Chapter 3

## Problem Definition

The definition of Pedestrian Dead-reckoning system is that to estimate the pedestrian's location is only with the pedestrian's self-contained sensor, such as accelerometers, magnetometers, gyroscopes, and altimeters, no external infrastructures. If we don't have a proper method to correct accumulated error, it's impossible to derive the displacement by acceleration integration with consumer level sensor. The drifting problem of sensor would cause system positioning accuracy divergence in a short time. The ZUPT is an effective and only method at present. But its limit is the inertial sensor that has to be installed on the foot. The side effect of the sensor installation on the foot is that the dramatic foot movement would obstruct acceleration measurement and heading determination. And the heading determination error would seriously affect the PDR localization performance. The objective of this thesis is to propose a new correction method, to avoid the defect of the ZUPT, and to design a new PDR system by the new method to implement and verify it.



# Chapter 4

## Methodology

An inherent limitation with most PDR solutions is the error drifting problem. The ZUPT PDR attacks this problem by resetting user's velocity to zero when it detects that the foot is standing on the floor. This requires the sensor be mounted on a foot, leading to a lot of vibrations and thus errors when measuring azimuths. To alleviate this problem, we propose our WUPT solution. See figure 4-1, the main idea is to use two inertial sensors SI and Sb mounted on the lower leg and the torso of the user respectively. Sb measures the user's walking velocity but is corrected by SI in every stride based on the angular velocity measured by SI happen on vertical straight line condition.

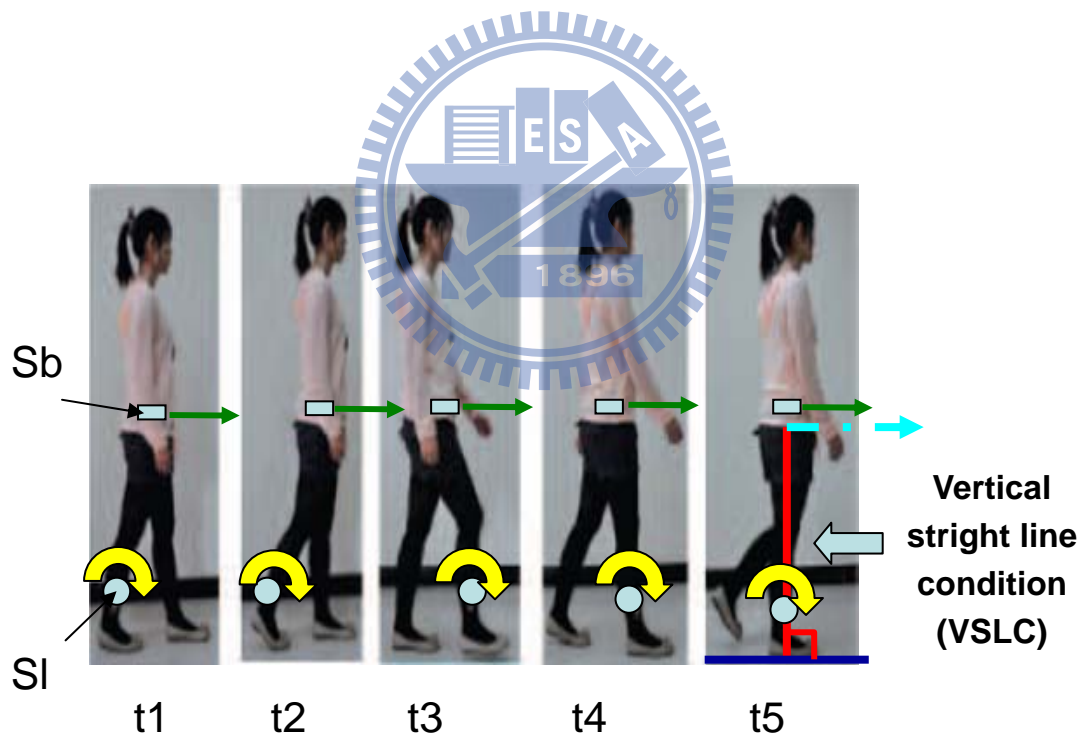


Figure 4-1 placement of inertial sensor Sb and SI

In the following article, first we will define coordinate systems we used, later the idea of the WUPT will be explained, and finally we will present a new PDR system, which is designed with the WUPT technique.

## 4.1 Coordinate Systems and Transformations

### 4.1.1 Local Level Frame (l-frame)

The local level frame is also called local geodetic or tangent frame. The local level frame has the north, east and down directions. See figure 4-2, the local level frame is attached to a fixed point on the surface of the earth at some convenient point for local measurements. This point is the origin of the local level frame. The x-axis points geographic north, y-axis points east and the z-axis complies with the right-handed coordinate system pointing toward that interior of the earth perpendicular to the reference ellipsoid.

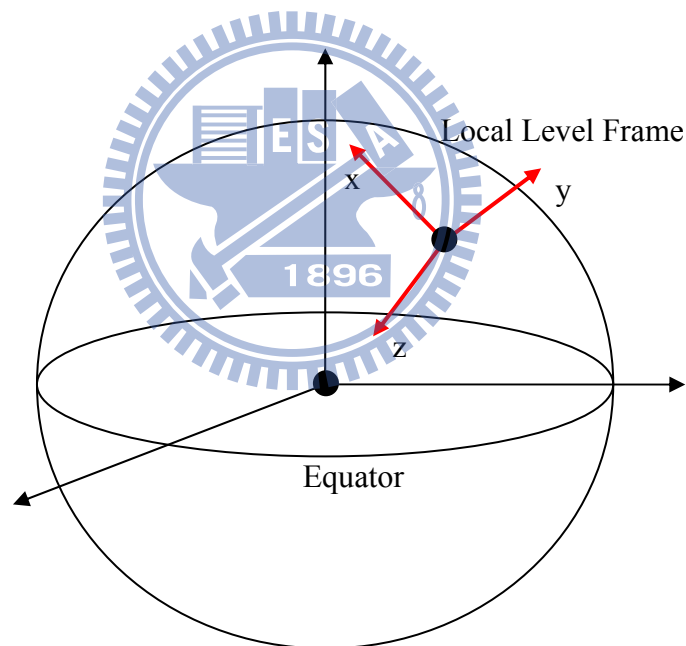


Figure 4-2 local level frame

We use the local level frame as the navigation frame to observe Pedestrian's motion

### 4.1.2 The Body Frame (b-frame)

The body frame is sometimes called the vehicle frame. See figure 4-3, the x-axis is defined in the forward direction, the z-axis is defined to pointing to the bottom of the user's foot and y-axis complies the right-handed orthogonal coordinate system.

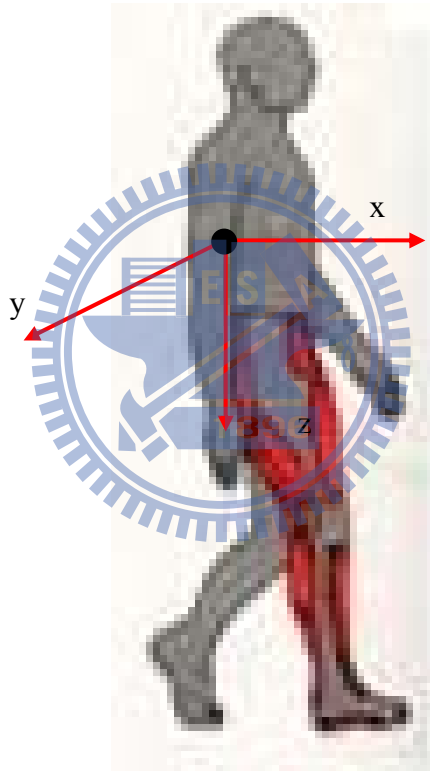


Figure 4-3 body frame

### 4.1.3 The Sensor Frame (s-frame)

The sensor frame is the coordinate system used by the sensor devices for sensor readings. The coordinate depends on the assembling of sensor ICs and devices calibration. The direction of x-axis, y-axis, and z-axis are indicated by hardware specs and follow the right hand rule. In our navigation application, the sensor frame is rigidly attached to the user and is aligned with the body frame.

### 4.1.4 Coordinate Frame Transformation

In our navigation application, the objectives are to determine the position of the user in local level frame, based on the measurements from the sensor frame attached to the user. So it is often necessary to transform a vector from one coordinate system into another coordinate system. There are three major methods can present the relationship between these frames, which are rotation matrix, direction cosine matrix, and quaternion. We will introduce the rotation matrix from sensor frame to local level frame. Rotation matrix can be defined by a series of three plane rotations involving Euler-angles ( $\Phi$ ,  $\theta$ ,  $\Psi$ ) and defined as (roll, pitch, and yaw). The first rotation is about the z-axis of the local level frame, which is rotated by  $\Psi$  radians. This rotation aligns the new x'-axis with the projection of x-axis of sensor frame into the local level frame, see Figure 4-4. The frame rotation is given by:

$$R(\psi) = \begin{bmatrix} \cos(\psi) & \sin(\psi) & 0 \\ -\sin(\psi) & \cos(\psi) & 0 \\ 0 & 0 & 1 \end{bmatrix} \quad (4.1)$$

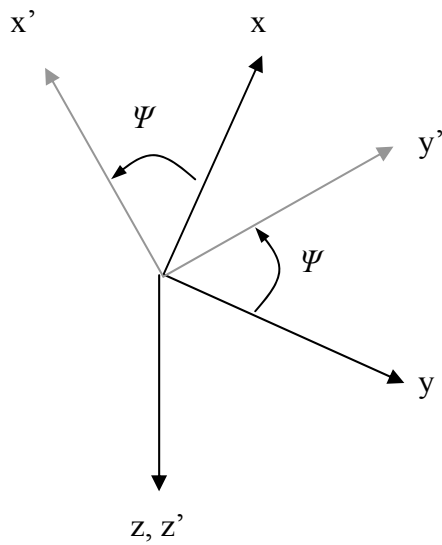


Figure 4-4 rotation 1

Next rotation rotates the coordinate system by  $\theta$  radians about the  $y'$ -axis. See figure 4-5, the rotation aligns the new  $x''$ -axis with the  $x$ -axis of sensor frame. For this operation the frame rotation is described as:

$$R(\theta) = \begin{bmatrix} \cos(\theta) & 0 & -\sin(\theta) \\ 0 & 1 & 0 \\ \sin(\theta) & 0 & \cos(\theta) \end{bmatrix} \quad (4.2)$$

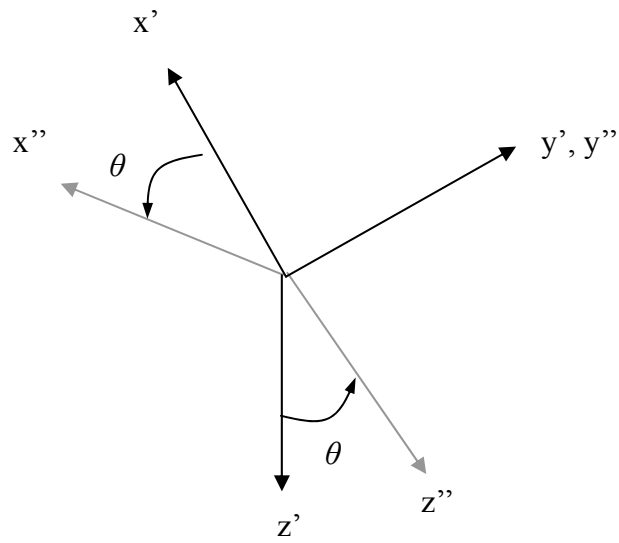
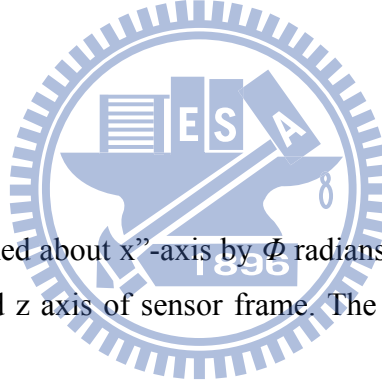


Figure 4-5 rotation 2



The third rotation is performed about  $x''$ -axis by  $\phi$  radians. See figure 4-6, this rotation aligns the new axes with the y and z axis of sensor frame. The frame rotation for this operation is described as:

$$R(\phi) = \begin{bmatrix} 1 & 0 & 0 \\ 0 & \cos(\phi) & \sin(\phi) \\ 0 & -\sin(\phi) & \cos(\phi) \end{bmatrix} \quad (4.3)$$

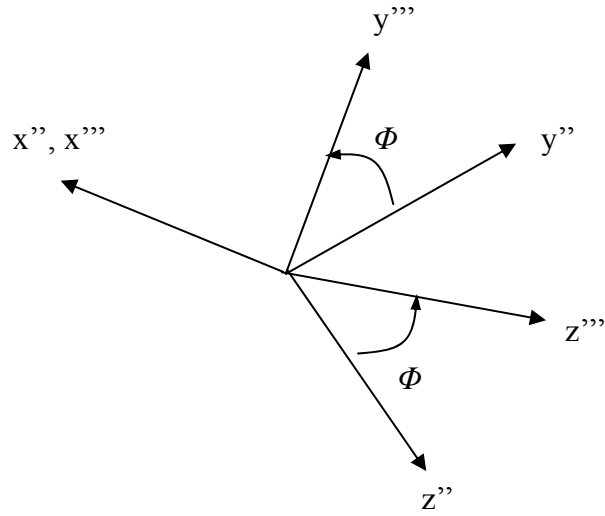


Figure 4-6 rotation 3

In this way, the local level frame coordinates can be transformed to the sensor frame coordinates by three rotations. The rotation matrix  $R_{l2s}$  can be found by multiplying all three rotations.

$$R_{l2s}(\psi, \theta, \phi) = R(\phi)R(\theta)R(\psi) \quad (4.4)$$

The transformed  $R_{l2s}$  gives the sensor to local level matrix,  $R_{s2l}$ , since  $R_{l2s}$  is a unitary matrix.

$$R_{l2s}(\psi, \theta, \phi) = R_{s2l}(\psi, \theta, \phi)^T = \begin{bmatrix} \cos(\psi) \cos(\theta) & \cos(\psi) \sin(\theta) \sin(\phi) - \sin(\psi) \cos(\phi) & \cos(\psi) \sin(\theta) \cos(\phi) + \sin(\psi) \sin(\phi) \\ \sin(\psi) \cos(\theta) & \sin(\psi) \sin(\theta) \sin(\phi) + \cos(\psi) \cos(\phi) & \sin(\psi) \sin(\theta) \cos(\phi) - \cos(\psi) \sin(\phi) \\ -\sin(\theta) & \cos(\theta) \sin(\phi) & \cos(\theta) \cos(\phi) \end{bmatrix} \quad (4.5)$$



## 4.2 WUPT Technique

The WUPT is short for the walking velocity update, which comes from the analysis of the human walking gait. First, we develop a kinematics model of human walking in mid-stance shown in Figure 4-7. The foot speed is vector  $V_{\text{foot}}$ , the knee speed is vector  $V_{\text{knee}}$ , the hip speed is vector  $V_{\text{hip}}$ , the speed at any point of the torso is vector  $V_{\text{ref}}$ , the lower leg angular speed is vector  $\Omega_{\text{lower\_leg}}$ , the upper angular speed is vector  $\Omega_{\text{upper}}$ , the torso angular speed is vector  $\Omega_{\text{torso}}$ , the lower leg length is vector  $L_{\text{lower\_leg}}$ , the upper length is vector  $L_{\text{upper}}$ , and the total leg length is vector  $L_{\text{leg}}$ .

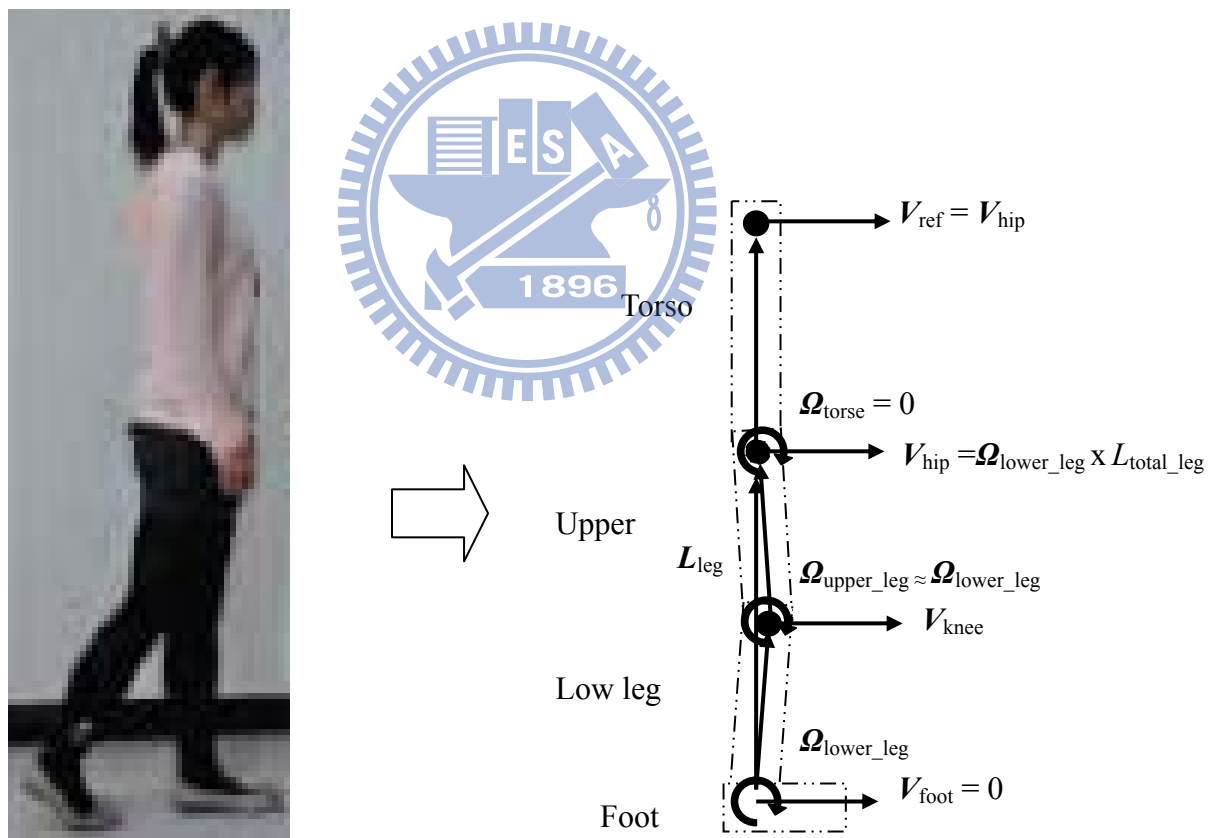


Figure 4-7 kinematics model of human walking in mid-stance

In walking, the motion of the knee is known as the knee flexion and extension (see Figure 4-8). This motion curve can be described as two flexion waves. Each of the flexion waves starts in relative extension, progresses into flexion, and then returns to the starting point in extension again. The first flexion wave, or stance phase knee flexion, peaks in early stance at opposite foot-off and back into extension by mid stance. The second flexion wave begins right after the heel rises to a maximum in swing phase as the swinging foot passes the opposite limb [21]. According to the experience, we can see the knee is at full extension status in the mid-stance, the upper and the lower leg have no relative rotation and form a straight line that is almost perpendicular to the ground. We call this *the vertical straight-line condition* (VSLC).

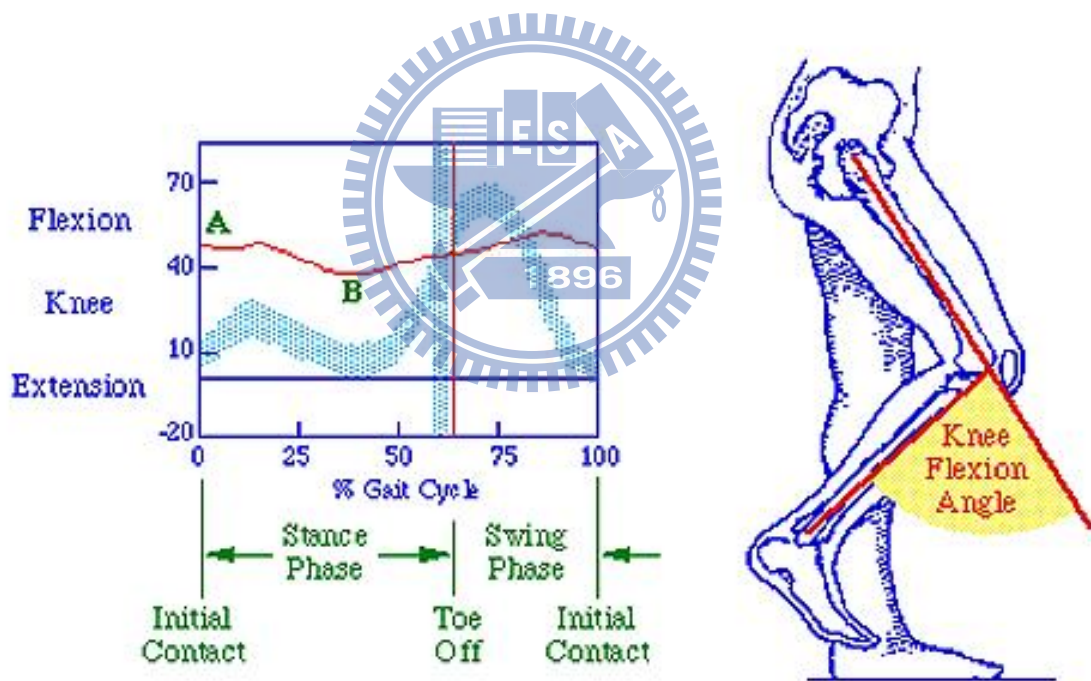


Figure 4-8 the motion curve of knee

In this condition:

⊖ the foot touches the ground, so  $V_{\text{foot}} = 0$

⊖ the upper and the lower leg have no relative rotation, so  $\Omega_{\text{upper\_leg}} = \Omega_{\text{lower\_leg}}$

$$\Rightarrow V_{\text{hip}} = V_{\text{foot}} + \Omega_{\text{lower\_leg}} \times L_{\text{lower\_leg}} + \Omega_{\text{upper\_leg}} \times L_{\text{upper\_leg}}$$

$$= \Omega_{\text{lower\_leg}} \times (L_{\text{lower\_leg}} + L_{\text{upper\_leg}})$$

$$= \Omega_{\text{lower\_leg}} \times L_{\text{total\_leg}} \quad (4.6)$$

⊖ the torso is almost up right from the ground due to the human walking behavior, so

$$\Omega_{\text{torse}} = 0$$

$$\Rightarrow V_{\text{ref}} = V_{\text{hip}} \quad (4.7)$$

⊖ the leg is almost perpendicular to the ground, so the vector  $V_{\text{hip}}$  and  $V_{\text{ref}}$ ,

$$\text{its magnitude } |V_{\text{hip}}| \text{ and } |V_{\text{ref}}| \text{ is } \omega_{\text{lower\_leg}} l_{\text{total\_leg}} \quad (4.8)$$

its direction is horizontal to the ground

We place a sensor Sb, which is attached to the user's upper body, to track pedestrian velocity derived by the acceleration and another sensor Sl attached to the user's lower leg measuring angular rate. We track the timing of *the vertical straight-line condition* from each step, obtain a reference velocity from Sl to correct the pedestrian moving velocity deduced by acceleration of Sb. These are the principals of the WUPT technique. Because the change of the moving of Sl which is installed on the torso is milder, and the acceleration and azimuth that we measured is more reliable, we can expect that the PDR system of the WUPT has superior positioning performance than the ZUPT.

### 4.3 WUPT PDR System Architecture

Now we design the new PDR system with the WUPT technique. The function block of the WUPT PDR is shown as Figure 4-9. A torso-mounted Sb consists of a triaxial accelerometer, a triaxial e-compass, and a triaxial gyroscope. A leg-mounted SI also consists of a triaxial accelerometer, a triaxial e-compass, and a triaxial gyroscope. The Raw Data Processing block for Sb will extract acceleration and orientation information from Sb’s sensing data. The Raw Data Processing block for SI will extract pitch  $\theta_{\text{lower\_leg}}$  and angular velocity  $\omega_{\text{lower\_leg}}$  from SI’s sensing data. The Stride Detection block uses the pitch value  $\theta_{\text{lower\_leg}}$  and angular velocity  $\omega_{\text{lower\_leg}}$  to determine *the vertical straight-line condition (VSLC)*. When *the vertical straight-line condition* is happening, the stride detection block will trigger a stride event. Then the Walking Velocity Update block will compute the torso’s reference velocity  $\omega_{\text{lower\_leg}} l_{\text{leg}}$  and report this velocity to the Location Tracking block. The Location Tracking block then corrects its magnitude of pedestrian estimated speed  $V_p$  as  $\omega_{\text{lower\_leg}} l_{\text{leg}}$  and starts computing the stride length and its direction by integrating its sensed acceleration (from Sb) over time until the next stride event is reported. At the end, the sum of each stride vector is considered as the user’s trajectory. The descriptions of the function blocks are :

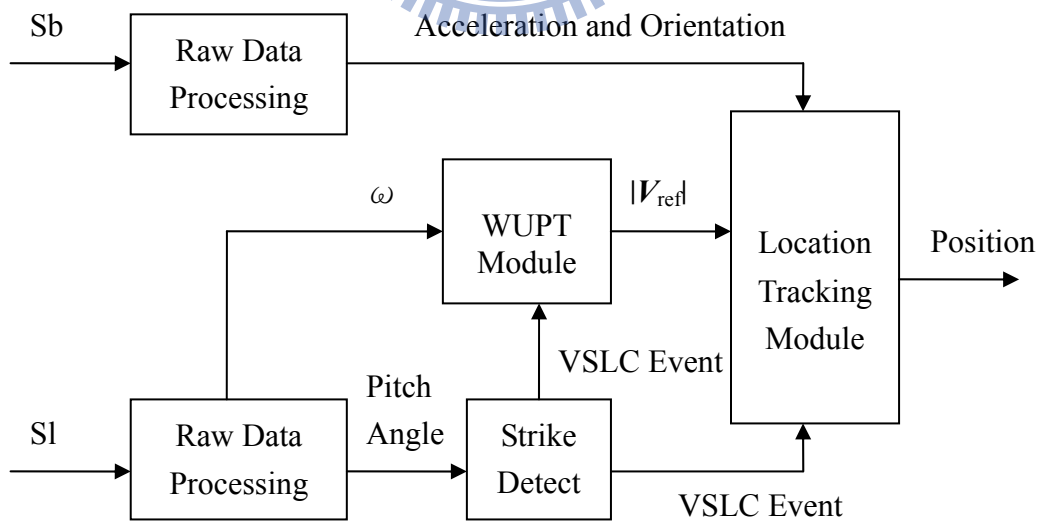


Figure 4-9 function block of WUPT PDR

## 4.2.1 Stride Detection Block

The most critical issue in the WUPT is to find a good point – *the vertical straight-line condition* to correct the user’s walking velocity. Consider the snapshots of five postures in a stride that we took from two users in Figure 4-10. In both cases, during the fifth to the sixth posture, the pitch angle of lower leg will gradually reduce from a negative value to a positive value. At the point when its value becomes zero, meet *the vertical straight-line condition*.

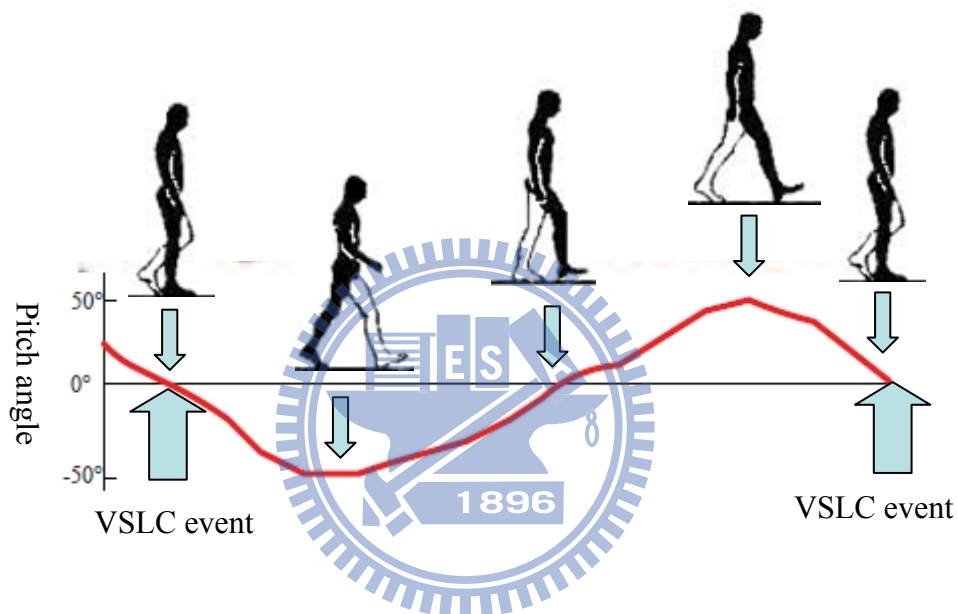


Figure 4-10 A stride cycle of human walking

According to our experiment that *the vertical straight-line condition* also happens in the local minimum area of angular velocity curve of lower leg, see Figure 4-11. We can also distinguish *the vertical straight-line condition* by monitoring the change of the angular velocity of lower leg, and apply that as augment method. When it detects *the vertical straight-line condition*, a trigger will be sent to both the Walking Velocity Update block and the Location Tracking block.

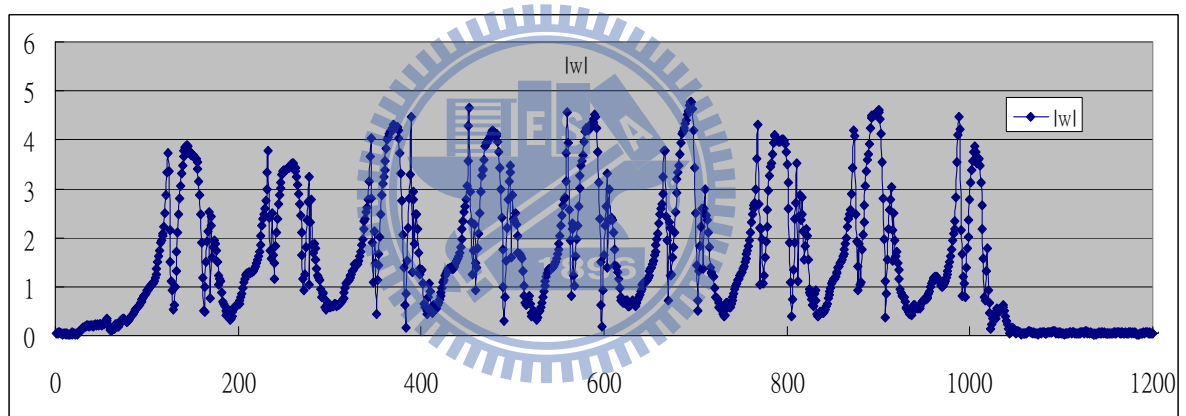
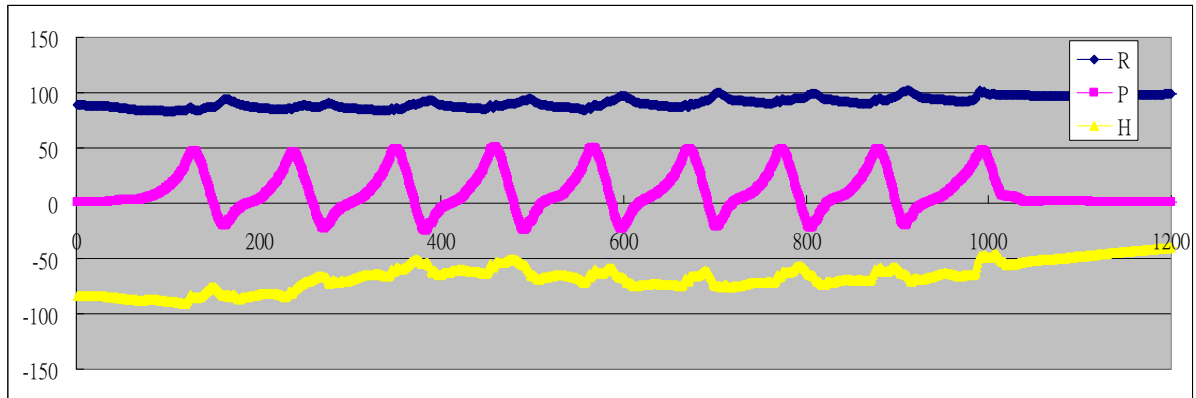


Figure 4-11 a chart of pitch angle and angular rate of lower leg with time

## 4.2.2 Walking Velocity Update Block

When *the vertical straight-line condition* event report is sent to the Walking Velocity Update block, the angular velocity  $\omega_{\text{lower\_leg}}$  of S1 and length  $l_{\text{leg}}$  of leg will be used to find reference velocity of pedestrian of the current stride. Note that we use moving average filtering to obtain a smooth value of  $\omega_{\text{lower\_leg}}$ .

## 4.2.3 Location Tracking Block

When a stride event is reported to the Location Tracking block, it will start to compute the next stride length and its direction by integrating Sb's acceleration and orientation during that stride until the next stride event is reported. The algorithm is as follows:

Let inertial sensor Sb sample period is  $\Delta t$ , in stride  $i$  time  $k$ , the measured azimuth relative to local frame can be present by  $\Psi^i[k], \Phi^i[k], \theta^i[k]$ , the measured component of acceleration relative to sensor frame  $(x, y, z)$  can be present as  $(a_x^i[k], a_y^i[k], a_z^i[k])$ , so the acceleration  $A^i[k]$  relative to local frame  $(n, e, d)$  can be presented as  $(a_n^i[k], a_e^i[k], a_d^i[k])$ , and we can get

$$\begin{bmatrix} a_n^i[k] \\ a_e^i[k] \\ a_d^i[k] \end{bmatrix} = R_{l2s} \begin{pmatrix} \psi^i[k] \\ \phi^i[k] \\ \theta^i[k] \end{pmatrix} \times \begin{bmatrix} a_x^i[k] \\ a_y^i[k] \\ a_z^i[k] \end{bmatrix}, \quad (4.8)$$

where the rotation matrix  $R_{l2s}(\psi, \theta, \phi)$  is equation (4-5)

According to Newton's motion equation, the pedestrian speed  $V^i[k]$  can be presented as:

$$V^i[k] = V^i[0] + \sum_0^k A^i[m] \Delta t \quad (4.9)$$

Where  $V^i[0]$  is the initial speed, its magnitude is determined by stride  $i$  reference velocity  $w_{\text{lower\_leg}}^i l_{\text{leg}}$  which comes from the WUPT module, so the walking speed can be calculated as:

$$\begin{aligned}
v_n^i[k] &= w_{lower\_leg}^i l_{total\_leg} \cos(\psi^i[0]) + \sum_{m=0}^k a_n^i[m] \Delta t \\
v_e^i[k] &= w_{lower\_leg}^i l_{total\_leg} \sin(\psi^i[0]) + \sum_{m=0}^k a_e^i[m] \Delta t
\end{aligned} \tag{4.10}$$

Note that we take the orientation measurement of Sb as heading determination.

And the current stride reference velocity  $\omega_{lower\_leg}^i l_{leg}$  can be used to correct the sensor accumulated error of previous stride. Here we only use the simple linear compensation method to fix  $V_n^{i-1}[k]$  as:

$$\begin{aligned}
v_n^{i-1}[k]_{after} &= v_n^{i-1}[k] + k * (w_{lower\_leg}^i l_{leg} \cos(\psi^i[0]) - v_n^{i-1}[T^i]) / T^i \\
v_e^{i-1}[k]_{after} &= v_e^{i-1}[k] + k * (w_{lower\_leg}^i l_{leg} \sin(\psi^i[0]) - v_e^{i-1}[T^i]) / T^i
\end{aligned} \tag{4.11}$$

Where the period  $T^i$  of stride  $i$  is the time between previous stride  $i-1$  event tick and the current stride  $i$  event tick.

Then the displacement  $\Delta S_n^{i-1}$  ( $\Delta s_n^{i-1}, \Delta s_e^{i-1}$ ) of stride  $i-1$  can be calculated as:

$$\begin{aligned}
\Delta s_n^{i-1} &= \sum_{k=0}^{T^{i-1}} v_n^{i-1}[k]_{after} \Delta t \\
\Delta s_e^{i-1} &= \sum_{k=0}^{T^{i-1}} v_e^{i-1}[k]_{after} \Delta t
\end{aligned} \tag{4.12}$$

Finally, the pedestrian position  $P^i(p_n^i, p_e^i)$  after stride  $i$  can be estimated as:

$$\begin{aligned}
p_n^i &= \sum_{j=0}^{i-1} \Delta s_n^j \\
p_e^i &= \sum_{j=0}^{i-1} \Delta s_e^j
\end{aligned} \tag{4.13}$$

Above is the explanation of the PDR with the WUPT design. The design is superior to the ZUPT PDR due to the torso-mounted inertial sensor. By that we can obtain more accurate and more reliable acceleration measurements and the heading-direction determinations; meanwhile, we can also expect more accurate tracking results for the complicated pedestrian trajectory.



# Chapter 5

## Implementation and Experimentation

### 5.1 Implementation

In the implementation of the WUPT PDR, we use 3GM-DX1 (see Figure 5-1) as two inertial sensors, as shown in the following picture. The specification of 3GM-DX1 is as the following Table 5-1, each has triaxial gyroscope, magnetometer, and accelerometer can report acceleration, angular speed, and azimuth of sensor frame.

Orientation range (pitch, roll, yaw)	360° all axes (orientation matrix, quaternion) ± 90°, ± 180°, ± 180° (Euler angles)
Sensor range	gyros: ± 300°/sec FS accelerometers: ± 5 g FS magnetometers: ± 1.2 Gauss FS
A/D resolution	16 bits
Accelerometer nonlinearity	0.2%
Accelerometer bias stability*	0.010 g
Gyro nonlinearity	0.2%
Gyro bias stability*	0.7°/sec
Magnetometer nonlinearity	0.4%
Magnetometer bias stability*	0.010 Gauss
Orientation resolution	<0.1° minimum
Repeatability	0.20°
Accuracy	± 0.5° typical for static test conditions ± 2.0° typical for dynamic (cyclic) test conditions & for arbitrary orientation angles
Digital output rates	100 Hz for Euler, Matrix, Quaternion 350 Hz for nine orthogonal sensors only
Weight (grams)	75 grams with enclosure, 30 grams without enclosure
Enclosure (w/tabs)	64 mm x 90 mm x 25 mm

Table 5-1 3GM-DX1 spec

We install one of the sensors on the waist (torso) and the other on the lower leg, and transmit the measurement data through the RS232 cable to a notebook (See Figure 5-2, 5-3, 5-4).



Figure 5-1 3DM-GX1



Figure 5-2 Sb placement



Figure 5-4 WUPT PDR



Figure 5-3 Sl placement

We develop a program named read3DMGX1.vi (see Figure 5-5) in the notebook monitoring and collecting sensor data and configure sample rate 75Hz and baud rate 38400 bps.

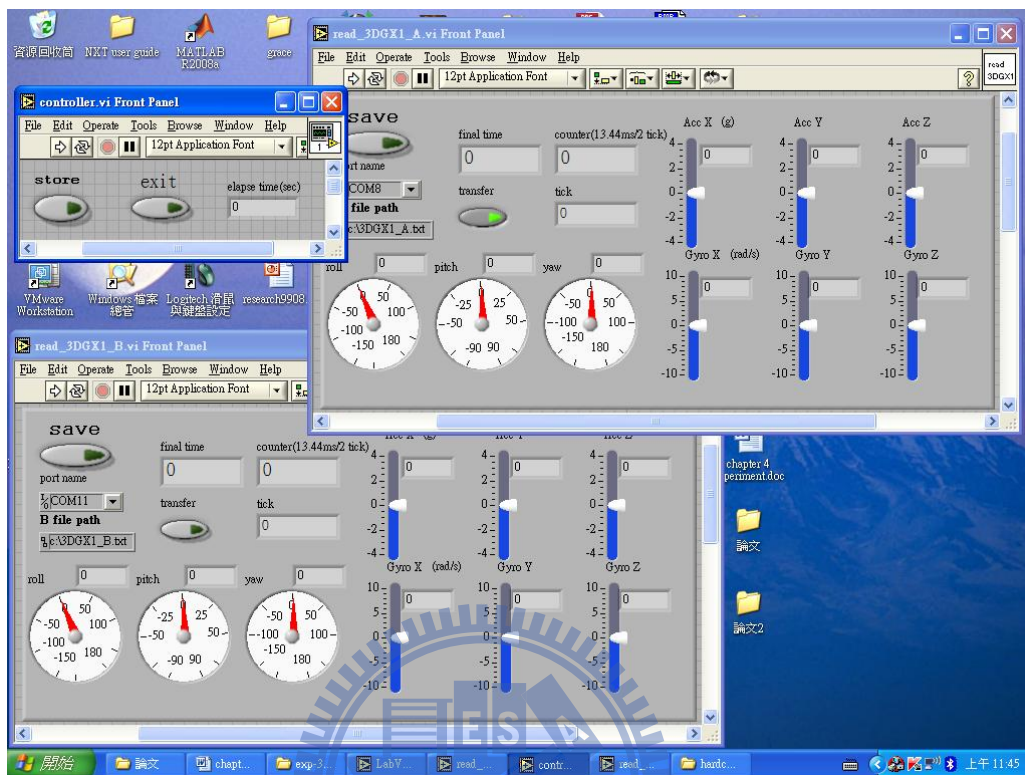


Figure 5-5 read3DMGX1.vi

Then we deal with data with another program named analysis.vi (See Figure 5-6) by post processed method after collecting all the experiment data. First we analyze the curve of the angular rate and the pitch azimuth from sensor S1 to obtain the results of the vertical straight line event tick and reference velocity. Later we estimate the pedestrian displacement and the trajectory tracking.

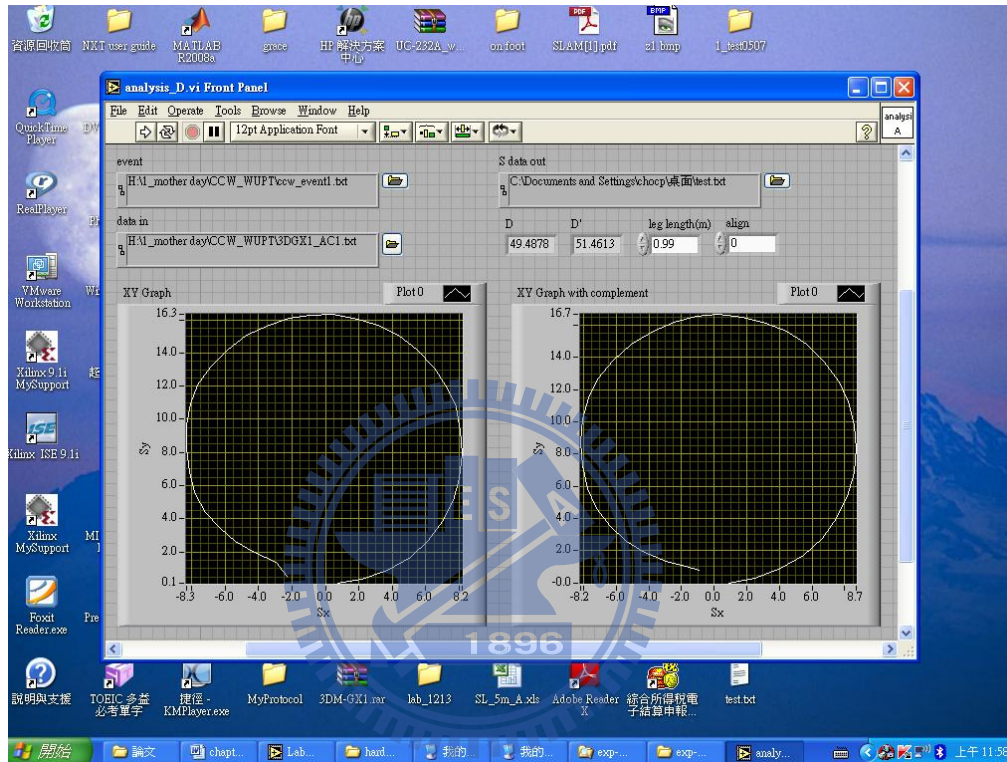


Figure 5-6 analysis.vi

## 5.2 Experimentation

First we chose a non-magnetic disturbance open space to do the straight-line walking test so that we could have a basic understanding of the WUPT PDR. Later we designed a square and a circle walking route to understand the positioning characteristics of the system and to compare with the ZUPT PDR. And we also did tests for the actual routes that people would take indoors and outdoors in order to understand the WUPT PDR positioning performance in practice.

### 5.2.1. Experiment 1 – The Basic Route Test

We chose a non-magnetic disturbance open space to do a 28 m long straight-line walking test in both high and low speeds. The result of the tests summary as Table 5-2 and the trajectory tracking are shown in Figure 5-7.

	Slow speed	Fast speed
Target distance	28m	28m
Cost time	34.0 sec	19.9 sec
Average velocity	0.82 m/s	1.41 m/s
Stride counts	23	17
Leg length	0.98 m	0.98 m
Estimate distance	29.0 m	27.0 m
Distance error	+3.6 %	-3.6 %
Heading error	3°	4°

Table 5-2 results of the basic test

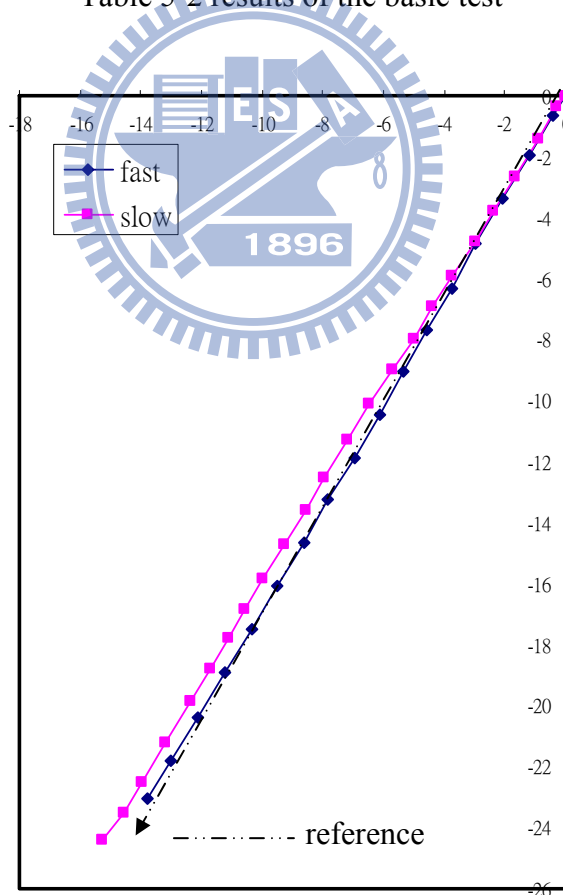


Figure 5-7 trajectory of the basic test

In Figure 5-8, we can observe the estimated velocity comparison before and after the WUPT update. If we infer the velocity from integrating acceleration without any correction method, you will get an unreasonable, even opposite data.

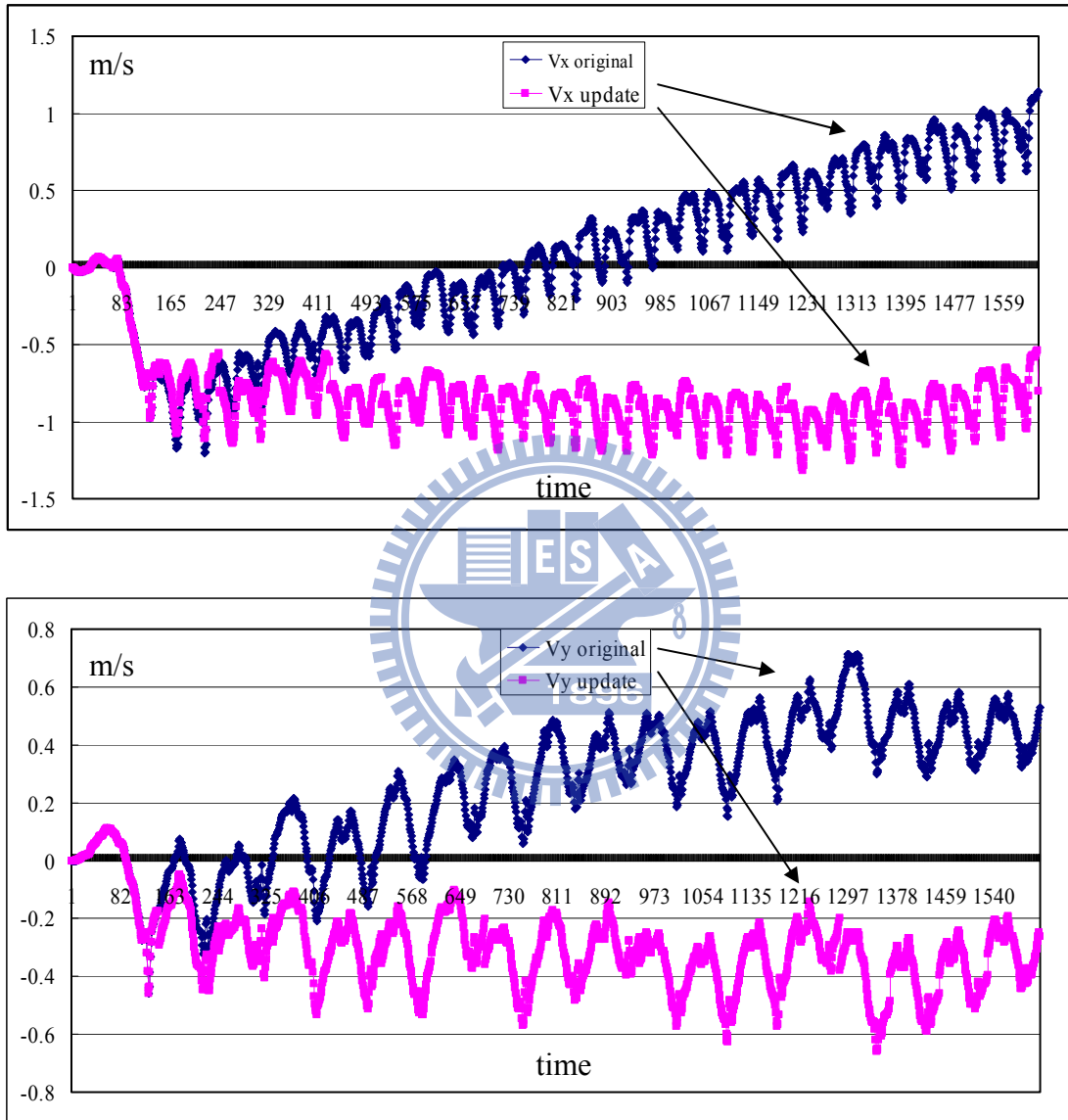


Figure 5-8 estimated velocity before and after WUPT update

The heading error in the estimation is under 0.3 degrees per meter. We can see the results from Figure 5-9 and Figure 5-10, which are from the diagraph of curves of heading direction towards what was gauged by Sb. The beginning and the end of the heading direction (yaw azimuth) almost match the design of the straight-line movement. We also observed that the pedestrians would oscillate while walking. The faster they walk, the bigger the oscillation angle is, which is about  $\pm 2.5^\circ$  for lower speed and  $\pm 5^\circ$  for higher speed.

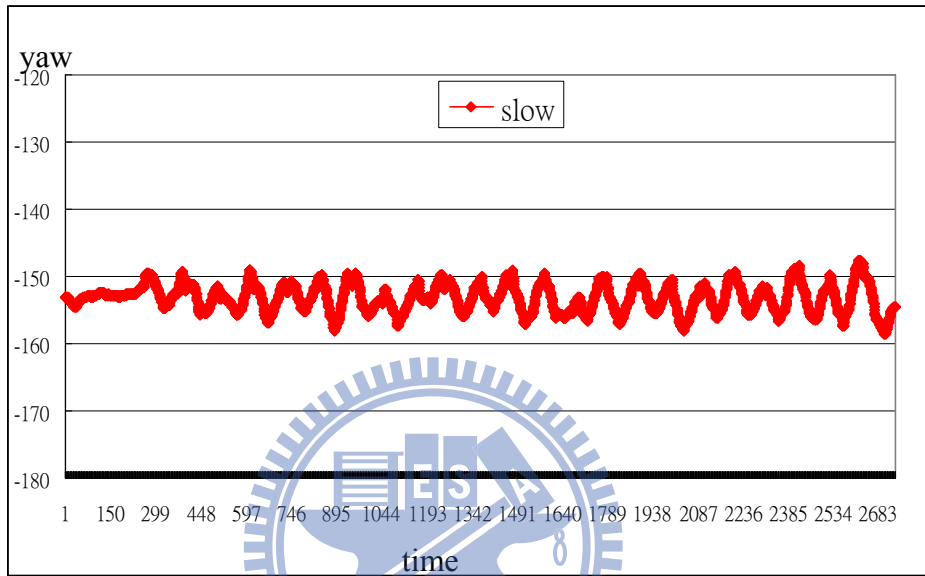


Figure 5-9 the measurement of heading direction on straight line at slow speed

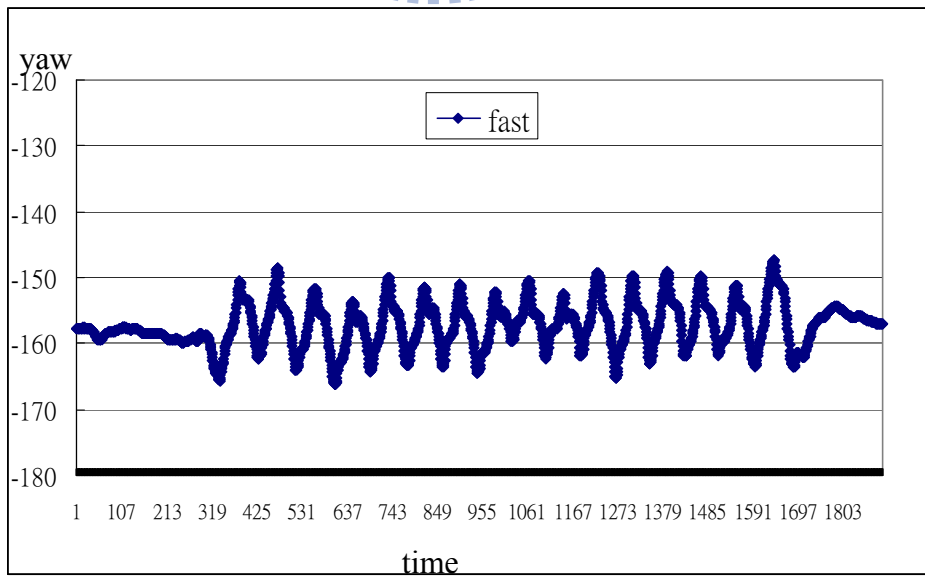


Figure 5-10 the measurement of heading direction on straight line at high speed

The distance estimation error is  $\pm 3.6\%$  and the sources of the errors come from the accuracy of the sensor, the timing error of detecting the vertical straight line condition, and there are design errors of the WUPT model that a human being's body is not rigid. While people are walking, the rotational motion would happen on the upper legs, lower legs and the hips. Those errors are regarded as noise for the system.

### **5.2.2. Experiment 2 – The Square Route Test**

We had this experiment at the outdoor basketball court in National Experimental High School at Hsinchu Science Park. The court is an open area, which faces south and leans toward east about  $8^\circ$ , and the length is 28 m and the width is 15 m. We walked along the basketball court (S1, S2, S3, S4) more than once to analyze the positioning characteristics of the WUPT and the ZUPT PDR. Here are the results, see Table 5-3, 5-4, Figure 5-11, 5-12.

We can tell that the trajectory tracking with the WUPT is closer to the practical walking route. It is also more accurate and stable than the ZUPT for the estimation of the heading direction and the distance. The reason is that the measurement data of the acceleration and azimuth changes more dramatically from the foot-mounted sensor than from the torso-mounted one.



		Displacement S1 L: 15m, H: 98°		Displacement S2 L: 28m, H: 188°		Displacement S3 L: 15m, H: 278°		Displacement S4 L: 28m, H: 8°		
Distance		length	error	length	error	length	error	length	error	statistics
	WUPT1	15.3m	2.2%	28.3m	0.9%	15.5m	3.6%	27.3m	2.7%	error
	WUPT2	15.1m	0.7%	26.5m	5.4%	16.1m	7.5%	28.2m	0.6%	Ave: 3.4%
	WUPT3	16.0m	7.1%	27.2m	3.1%	15.4m	2.6%	26.7m	4.6%	Sdev: 2.3%
Heading		angle	error	angle	error	angle	error	angle	error	statistics
	WUPT1	99.3°	1.3°	193.8°	5.8°	284.9°	6.9°	6.4°	1.6°	error
	WUPT2	96.9°	1.1°	194.9°	6.9°	283.2°	5.2°	5.7°	2.3°	Ave: 3.9°
	WUPT3	95.3°	2.7°	193.0°	5.0°	286.2°	8.1°	8.0°	0°	Sdev: 2.7°

Table 5-3 results of WUPT of the Square Route test

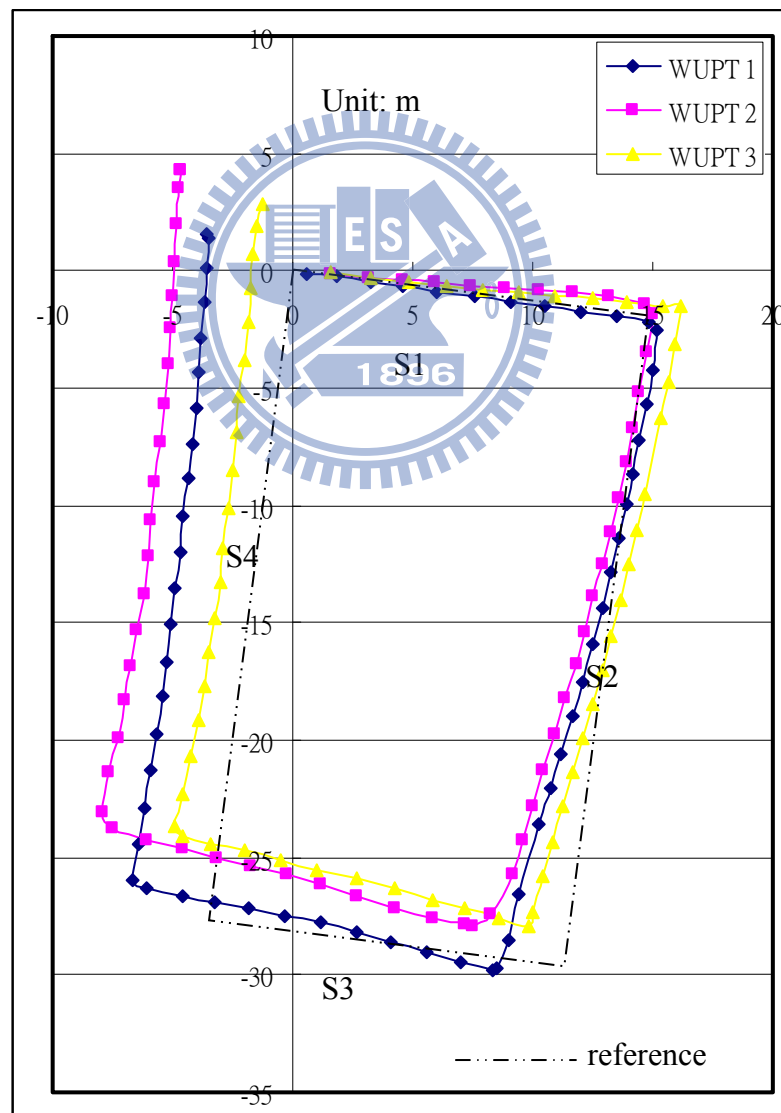


Figure 5-11 trajectory of WUPT of the Square Route test

		Displacement 1 L: 15m, H: 98°		Displacement 2 L: 28m, H: 188°		Displacement 3 L: 15m, H: 278°		Displacement 4 L: 28m, H: 8°		
Distance		length	error	length	error	length	error	length	error	statistics
	ZUPT1	11.0m	26.2%	21.3m	23.9%	13.1m	12.9%	24.7m	11.9%	error
	ZUPT 2	12.8m	14.6%	22.3m	20.3%	13.4m	10.6%	25.3m	9.7%	Ave: 14.1%
	ZUPT 3	14.1m	5.6%	22.8m	18.4%	14.3m	4.9%	25.3m	9.8%	Sdev: 6.9%
Heading		angle	error	angle	error	angle	error	angle	error	statistics
	ZUPT 1	94.0°	23.0°	200.8°	12.8°	288.2°	10.1°	5.1°	2.8°	error
	ZUPT 2	86.6°	11.4°	178.4°	9.6°	275.8°	2.2°	6.4°	1.6°	Ave: 6.4°
	ZUPT 3	89.6°	8.3°	179.6°	8.4°	274.8°	3.1°	6.0°	2.0°	Sdev: 4.1°

Table 5-4 results of ZUPT of the Square Route test

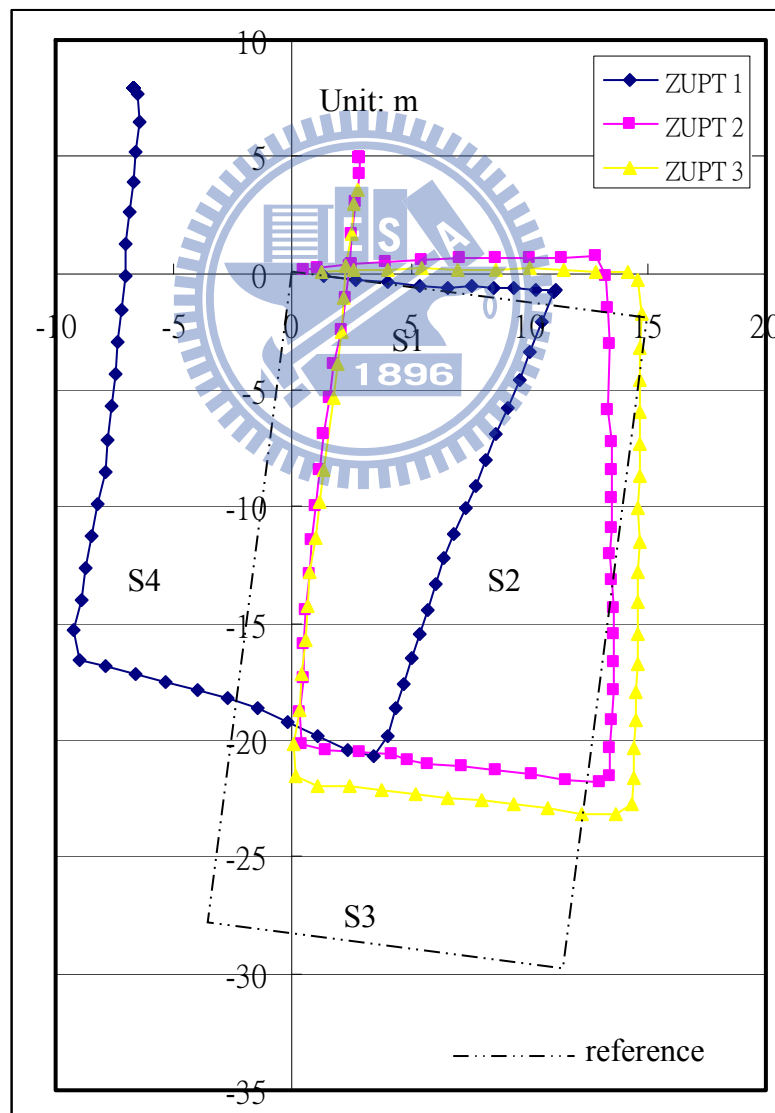
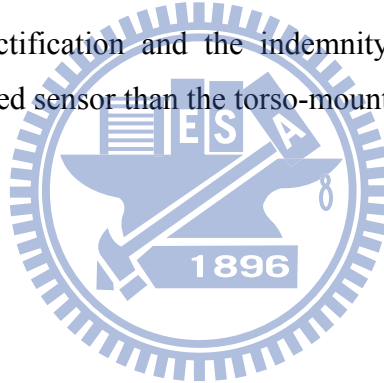


Figure 5-12 trajectory of ZUPT of the Square Route test

### 5.2.3. Experiment 3 – The Circle Route Test

The test environment is located at the roundabout of the Science Park Administration. The diameter of the roundabout is 16 m. We walked clockwise along it more than once in order to trace the pedestrian's walking trajectory, to test the positioning characteristics of the WUPT PDR, and to compare it with the ZUPR PDR. Here are the results, see Table 5-5, 5-6, Figure 5-13, 5-14.

We can tell that the trajectory tracking with the WUPT technique is closer to the practical walking route. It is also more accurate and stable than the ZUPT for the estimation of the heading direction and the distance. We also compared the pedestrian tracking trajectory of the WUPT PDR with the WUPT PDR before they were rectified. The data of the tracking from both systems without rectification became worthless within a short distance, which shows the importance of the error rectification and the indemnity method. Also we can see more deviation for the foot-mounted sensor than the torso-mounted one.



		Reference	Estimate	Error
WUPT1	Distance	50.3 m	51.0 m	1.4%
	Final Location	(N : 0 m, E : 0 m )	(N : -0.9 m, E : 0.8 m)	1.2 m
WUPT2	Distance	50.3 m	51.9 m	3.3%
	Final Location	(N : 0 m, E : 0 m )	(N : -0.6 m, E : 0.7 m)	0.9 m
WUPT3	Distance	50.3 m	51.8 m	2.7%
	Final Location	(N : 0 m, E : 0 m )	(N : -1.0 m, E : -0.3 m)	1.0 m

Table 5-5 results of WUPT of the Circle Route test

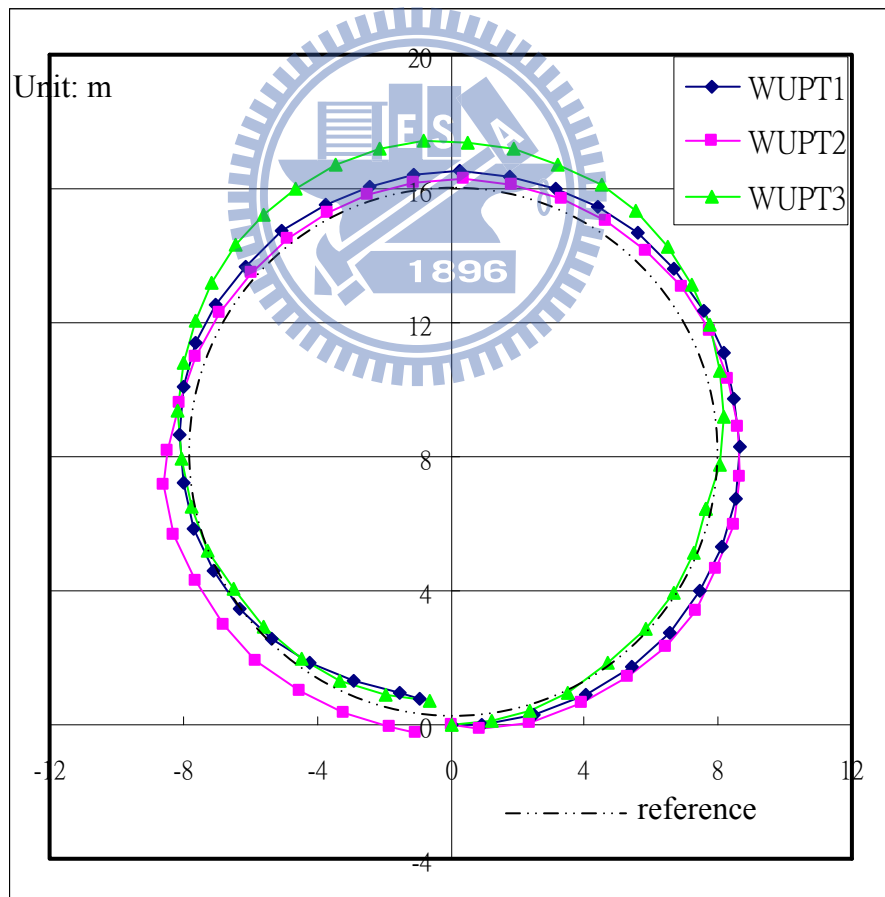


Figure 5-13 trajectory of WUPT of the Circle Route test

		Reference	Estimate	Error
ZUPT1	Distance	50.3 m	53.9 m	7.1%
	Final Location	(N : 0 m, E : 0 m )	(N : -0.3 m, E : 0.7 m)	0.7 m
ZUPT2	Distance	50.3 m	50.5 m	0.3%
	Final Location	(N : 0 m, E : 0 m )	(N : -3.0 m, E : 2.5 m)	3.9 m
ZUPT3	Distance	50.3 m	53.8 m	7.0%
	Final Location	(N : 0 m, E : 0 m )	(N : -0.1 m, E : 0.0 m)	0.1 m

Table 5-6 results of ZUPT of the Circle Route test

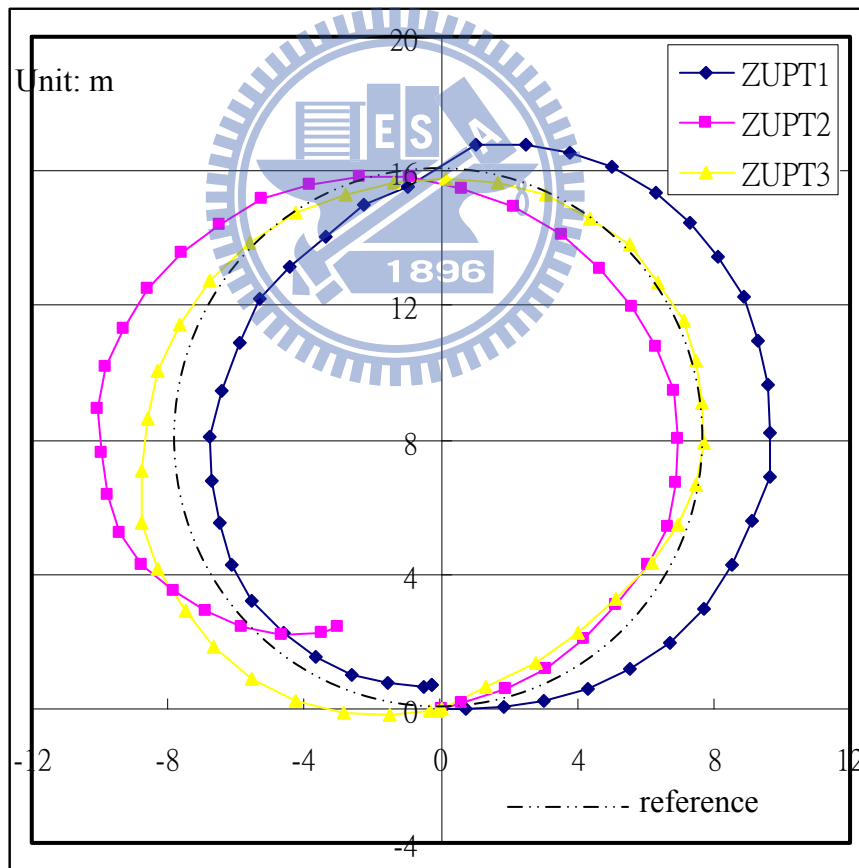


Figure 5-14 trajectory of ZUPT of the Circle Route test

## 5.2.4 Experiment 4 - The Practical Outdoor Positioning Test

The test occurred at the Bamboo Lake in National Chiao Tung University. The size of the lake is 130 m in length and 130 m in width. We simulated that the pedestrian walk counter-clockwise along the lake once and started from the platform, walked on the stairs and a hill at the corner on the left. The results of the WUPT PDR are as follows, Table 5-7, Figure 5-15.

	Reference	Estimate	Error
Distance	508 m	472.6 m	6.9%
Final Location	(N : 0 m, E : 0 m )	(N : 4.18 m, E : -22.8 m)	22.9 m

Table 5-7 results of the Practical Outdoor Positioning Test



Figure 5-15 trajectory of the Practical Outdoor Positioning Test

We can conclude that the accuracy of direction determination and distance estimation is high. The stairs and hills on the route would increase the positioning errors. We should consider the elements of the landscapes in the future.

### 5.2.5 Experiment 5 - The Practical Indoor Positioning Test

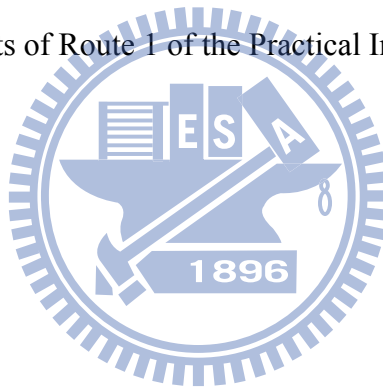
The site is located on the fifth floor in the third Engineering Building in National Chiao Tung University. We planned two possible routes for simulating pedestrian's tour:

#### Route 1:

The pedestrian departs from the elevator has a rest in the living room, reads in the conference room, comes back to the stairs and then leaves. The pedestrian trajectory tracked by the system is as follows:

	Reference	Estimate	Error
Distance	70 m	74.6 m	6.6%
Final Location	(N : -29 m , E : -27 m )	(N : -31.8m , E : -29.4 m )	3.7 m

Table 5-8 results of Route 1 of the Practical Indoor Positioning Test





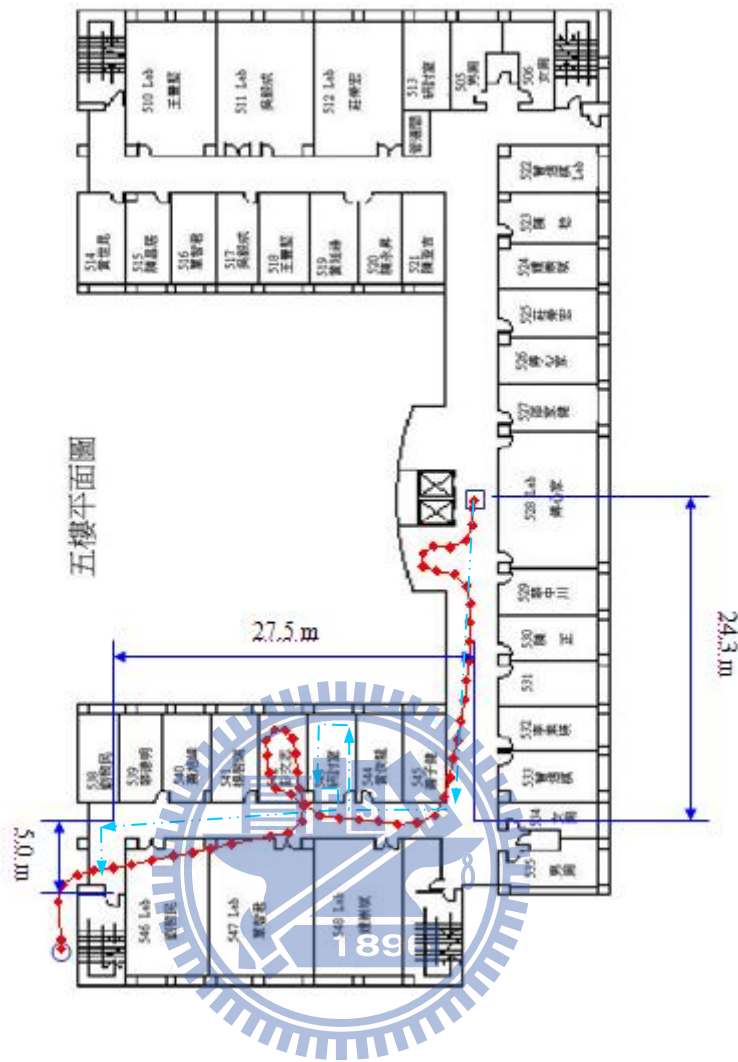


Figure 5-16 trajectory of Route 1 of the Practical Indoor Positioning Test

We discovered that the movement direction estimation indoors is less accurate than outdoors. We suspect that the electrical devices interfere with the sensor somehow. The tracking trajectory showed that the final location of the pedestrian was in the room next door. The positioning indoors is worse than outdoors.

### Route 2:

The pedestrian departs from the elevator and walks to the conference room and then reads there, walks to the stairs and is about to leave. The pedestrian decides to take the elevator instead and then leaves. The pedestrian trajectory tracked by the system is as follows

	Reference	Estimate	Error
Distance	124 m	121.2 m	2.2%
Location	(N : 0 m , E : 0 m)	(N : -1.7 m , E : -6.0 m)	6.2 m

Table 5-9 results of Route 2 of the Practical Indoor Positioning Test

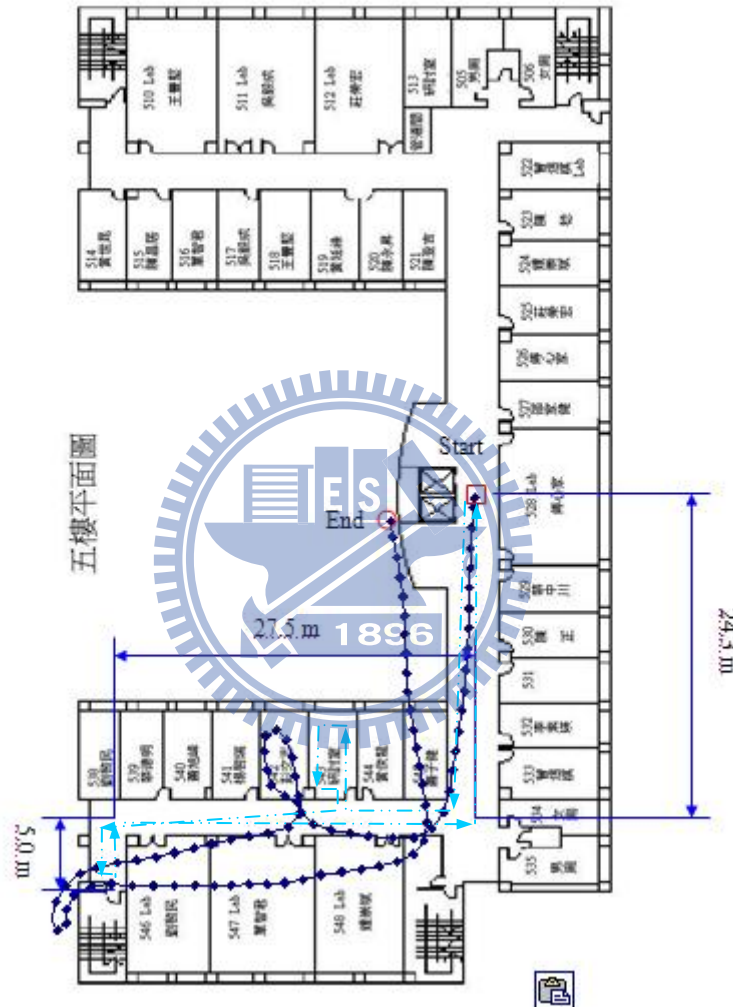


Figure 5-17 trajectory of Route 2 of the Practical Indoor Positioning Test

We discovered that the first part of the trajectory from the elevator to the stairs is more repetitive than in circumstance 1. The positioning function indoors is worse than outdoors

# Chapter 6

## Conclusion

To summarize, we have proposed a self-calibrated PDR solution with two inertial sensors mounted on a pedestrian. Sensor Sb is attached to the user's torso and sensor Sl attached to the user's lower leg. A novel concept called "Walking Velocity" Update has been proposed, where we use sensor Sl to find a good point to calibrate the user's walking velocity. Then, we use sensor Sb to track the user's velocity and orientation. In every stride, WUPT will extract pitch and angular velocity from Sl's sensing data and will detect *the vertical straight-line condition*. On happening of *the vertical straight-line condition*, the system calibrates its walking velocity by angular velocity. It also computes the stride length and its direction by integrating its sensed acceleration (from Sb) over time until the next *vertical straight-line condition* event is reported. At the end, the sum of each stride length and its orientation is considered as the user's trajectory. According to our experiments, the WUPT method is better than the ZUPT method.

# References

- [1] E. Foxlin, “Pedestrian tracking with shoe-mounted inertial sensors,” *Computer Graphics and Applications, IEEE*, vol. 25, no. 6, pp. 38 – 46, 2005.
- [2] L. Ojeda and J. Borenstein, “Personal dead-reckoning system for gps denied environments,” in *Safety, Security and Rescue Robotics, 2007. SSRR 2007. IEEE International Workshop on*, 2007, pp. 1 –6.
- [3] S.-P. Kuo, S.-C. Lin, B.-J. Wu, Y.-C. Tseng, and C.-C. Shen, “GeoAds: A Middleware Architecture for Music Service with Location-Aware Advertisement,” in *IEEE Int’l Conf. on Mobile Ad-hoc and Sensor Systems (MASS)*, 2007.
- [4] C.-C. A. Lo, T.-C. Lin, Y.-C. Wang, Y.-C. Tseng, L.-C. Ko, , and L.- C. Kuo, “Using intelligent mobile devices for indoor wireless location tracking, navigation, and mobile augmented reality,” in *IEEE VTS Asia Pacific Wireless Commun. Symposium (APWCS)*, 2010.
- [5] D. Niculescu and B. Nath, “Ad Hoc Positioning System (APS) Using AOA,” in *IEEE INFOCOM*, vol. 3, 2003, pp. 1734–1743.
- [6] M. Addlesee, R. Curwen, S. Hodges, J. Newman, P. Steggles, A. Ward, and A. Hopper, “Implementing a Sentient Computing System,” *Computer*, vol. 34, no. 8, pp. 50–56, 2001.
- [7] A. Savvides, C.-C. Han, and M. B. Strivastava, “Dynamic Fine-Grained Localization in Ad-Hoc Networks of Sensors,” in *ACM/IEEE MOBICOM*, 2001, pp. 166–179.
- [8] J. Zhou, K.-K. Chu, and J.-Y. Ng, “Providing location services within a radio cellular network using ellipse propagation model,” in *Advanced Information Networking and Applications, 2005. AINA 2005. 19<sup>th</sup> International Conference on*, vol. 1, march 2005, pp. 559 – 564 vol.1.
- [9] P. Bahl and V. N. Padmanabhan, “RADAR: An In-building RF-based User Location and Tracking System,” in *IEEE INFOCOM*, vol. 2, 2000, pp. 775–784.
- [10] J. J. Pan, J. T. Kwok, Q. Yang, and Y. Chen, “Multidimensional Vector Regression for Accurate and Low-Cost Location Estimation in Pervasive Computing,” *IEEE Trans. on Knowledge and Data Engineering*, vol. 18, no. 9, pp. 1181–1193, 2006.
- [11] S.-P. Kuo and Y.-C. Tseng, “A Scrambling Method for Fingerprint Positioning Based on Temporal Diversity and Spatial Dependency,” *IEEE Trans. on Knowledge and Data Engineering*, vol. 20, no. 5, pp. 678–684, 2008.
- [12] C.-M. Su, J.-W. Chou, C.-W. Yi, Y.-C. Tseng, and C.-H. Tsai, “Sensor-aided personal

- navigation systems for handheld devices,” in *Proceedings of the 2010 39th International Conference on Parallel Processing Workshops*, ser. ICPPW '10. Washington, DC, USA: IEEE Computer Society, 2010, pp. 533–541. [Online]. Available: <http://dx.doi.org/10.1109/ICPPW.2010.78>
- [13] X. Yun, E. Bachmann, H. Moore, and J. Calusdian, “Self-contained position tracking of human movement using small inertial/magnetic sensor modules,” in *Robotics and Automation, 2007 IEEE International Conference on*, 2007, pp. 2526–2533.
- [14] S. Shin, C. Park, J. Kim, H. Hong, and J. Lee, “Adaptive step length estimation algorithm using low-cost mems inertial sensors,” in *Sensors Applications Symposium, 2007. SAS '07. IEEE*, 2007, pp. 1–5.
- [15] A. Jimenez, F. Seco, C. Prieto, and J. Guevara, “A comparison of pedestrian dead-reckoning algorithms using a low-cost mems imu,” in *Intelligent Signal Processing, 2009. WISP 2009. IEEE International Symposium on*, aug. 2009, pp. 37–42.
- [16] R. Stirling, J. Collin, K. Fyfe and G. Lachapelle, “An Innovative Shoe-Mounted Pedestrian Navigation System” , In *GNSS 2003, Graz, Austria, 22-25 April*, 2003, pp. 1-15.
- [17] H. Weinberg, “Using the ADXL202 in Pedometer and Personal Navigation Applications,” *Analog Devices AN-602 application Note*, 2002
- [18] J. Won Kim, H. Jin Jang, D.H. Hwang, Ch. Park, “A Step, Stride and Heading Determination for the Pedestrian Navigation System” , *Journal of Global Positioning Systems*, Vol. 3, No. 1-2: 273-279, 2004.
- [19] Ascher, C., Kessler, C., Wankerl, M., Trommer, G.F., "Using OrthoSLAM and Aiding Techniques for Precise Pedestrian Indoor Navigation," *Proceedings of the 22nd International Technical Meeting of The Satellite Division of the Institute of Navigation (ION GNSS 2009)*, Savannah, GA, September 2009, pp. 743-749.
- [20] J. Borestein, L. Ojeda and S. Kwanmuang, “Heuristic reduction of gyro drift in IMU-based personnel tracking system,” In *SPIE Defense, Security and Sensing Conference, April 13-17, Orlando, Florida, USA*.
- [21] Rose, James G Gamble, “Human Walking”, published by Willians & Wilkins 2006, pp 45

# Biography

## Experience:

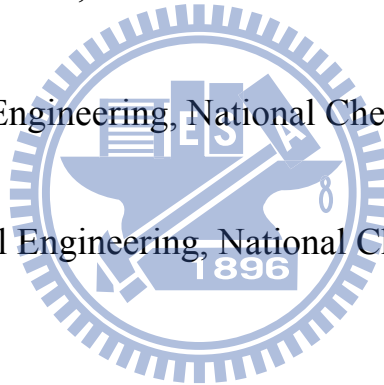
Research Engineer at PRINCO CORP. 1998 ~ now  
(machine design, embedded system design, testing design)

## Education:

Master, Computer Science, National Chiao Tung University, 2011

Master, Mechanical Engineering, National Cheng Kung University, 1996

Bachelor, Mechanical Engineering, National Cheng Kung University, 1994



## Contact information:

Office : No.6, Creation 4<sup>th</sup> Rd. Science-Based Industrial Park, Hsinchu,  
Taiwan, R.O.C

Email : [chocp.chiu@gmail.com](mailto:chocp.chiu@gmail.com)